This project has received funding from the Fuel Cells and Hydrogen 2 Joint Undertaking (now Clean Hydrogen Partnership) under grant agreement No 101006641. This Joint Undertaking receives support from the European Union's Horizon 2020 Research and Innovation programme, Hydrogen Europe and Hydrogen Europe Research.

IMPROVED LIFETIME STACKS FOR HEAVY DUTY TRUCKS THROUGH ULTRA-DURABLE COMPONENTS

Grant agreement no.: 101006641

***Start date**: 01.01.2021 – **Duration**: 42 months*

***Project Coordinator**: D. J. Jones, CNRS*

DELIVERABLE REPORT

D6.2: A FUEL CELL DEGRADATION MODEL FOR DURABILITY FORECASTING AND AN ALTERNATIVE APPROACH FOR LOAD PROFILE CREATION FOR DURABILITY TESTING	
Due Date	December 2023
Author (s)	Leonidas Tsikonis
Workpackage	WP 6, HD powertrain validation and system recommendations
Workpackage Leader	FPT Industrial
Lead Beneficiary	FPT Industrial
Date released by WP leader	07/02/2024
Date released by Coordinator	07/02/2024

DISSEMINATION LEVEL		
PU	*Public*	***X***
PP	*Restricted to other programme participants (including the Commission Services)*	
RE	*Restricted to a group specified by the consortium (including the Commission Services)*	
CO	*Confidential, only for members of the consortium (including the Commission Services)*	

NATURE OF THE DELIVERABLE		
R	*Report*	***X***
P	*Prototype*	
D	*Demonstrator*	

This project has received funding from the Fuel Cells and Hydrogen 2 Joint Undertaking (now Clean Hydrogen Partnership) under grant agreement No 101006641. This Joint Undertaking receives support from the European Union's Horizon 2020 Research and Innovation programme, Hydrogen Europe and Hydrogen Europe Research.

SUMMARY	
Keywords	*dynamic throughput, forecasting, degradation, durability, heavy-duty load profile test, Markov chain-based accelerated durability test*
Abstract	*Two new results produced by FPT in the framework of the project are presented in this report. A method for developing regression model for fuel cell degradation forecasting along with the necessary criteria for selection of the most appropriate model and a method for creating accelerated durability tests for fuel cells, based on Markov chains. Moreover, a correction in the definition of the Dynamic Throughput [1] is also given in the Appendix A.*
Public abstract for confidential deliverables	–

REVISIONS			
Version	**Date**	**Changed by**	**Comments**
0.1	20.12.2023	Leonidas Tsikonis	First draft.
0.2	22.01.2024	Leonidas Tsikonis	Corrections and editing. Correction of Table 1. Addition of paragraphs 3.2.4 and 3.2.5.
0.3	07.02.2024	Leonidas Tsikonis	Feedback from WP6 partners. Corrections. Addition of section 4.

This project has received funding from the Fuel Cells and Hydrogen 2 Joint Undertaking (now Clean Hydrogen Partnership) under grant agreement No 101006641. This Joint Undertaking receives support from the European Union's Horizon 2020 Research and Innovation programme, Hydrogen Europe and Hydrogen Europe Research.

A FUEL CELL DEGRADATION MODEL FOR DURABILITY TESTING AND AN ALTERNATIVE APPROACH FOR LOAD PROFILE CREATION FOR DURABILITY TESTING

CONTENTS

This project has received funding from the Fuel Cells and Hydrogen 2 Joint Undertaking (now Clean Hydrogen Partnership) under grant agreement No 101006641. This Joint Undertaking receives support from the European Union's Horizon 2020 Research and Innovation programme, Hydrogen Europe and Hydrogen Europe Research.

This project has received funding from the Fuel Cells and Hydrogen 2 Joint Undertaking (now Clean Hydrogen Partnership) under grant agreement No 101006641. This Joint Undertaking receives support from the European Union's Horizon 2020 Research and Innovation programme, Hydrogen Europe and Hydrogen Europe Research.

1 CONTEXT

The present deliverable report was originally intended to be an updated final version of the deliverable D6.1 ([1] submitted M12) with additional data from H2Haul project [2] field demonstration and eventually other HD and mobility applications [3]. Despite all efforts from the IMMORTAL and the H2Haul project management to obtain such data, the approach was fruitless.

In the meantime, during the project, a few notable results were obtained by FPT which were not originally foreseen during the preparation of the project proposal and therefore no relevant place was allocated in the list of deliverables. These results are:

a) the creation of a statistical fuel cell degradation model for durability forecasting, accounting for the operating conditions of the fuel cell, and
b) a new approach for the creation of load profiles for durability testing based on Markov chain stochastic processes.

Given that no additional data was available to produce the present deliverable as planned, the consortium agreed to use this report to announce and share the afore-mentioned new results that may be of public interest and at the same time be shared as results of the IMMORTAL project.

Further to the said announcement, the author wishes to make a correction in the definition of the dynamic throughput metric as introduced in [1]. This is done in the Appendix A (§6, p. 35).

2 A FUEL CELL DEGRADATION MODEL FOR DURABILITY FORECASTING

For the WP6 Tasks 6.2 (Projected performance and durability at system level) and 6.3 (Techno-economic validation of powertrain), the estimation of the fuel cells degradation is necessary for an assessment of a fuel cell truck's performance and total cost of ownership throughout its use. For this purpose, Bosch would provide relevant information from Task 2.4 (MEA extrapolated lifetime prediction – model based and empirical) in the form of "0D polarisation curves and/or functional maps of the IMMORTAL stack based on the new MEA" [3]. However, FPT came soon to the realisation that a more comprehensive modelling tool would be necessary for a more realistic estimation of the stack's behaviour and degradation as a function of its use history, which would be different under different vehicles, missions, operating conditions etc. (see also the modelling approach described in [1]).

Under the new understanding and given the important amount of experimental data from the LPT campaigns performed by Bosch, the author proceeded to the creation of a model alternative to the semi-empirical that Bosch employed. An outline of this modelling approach is the subject of the current section. The new model is based on the baseline stack which despite lower performance demonstrated better durability compared to other tested stacks [4].

2.1 Model structure

2.1.1 Available data

Bosch implemented several series of load profile testing (LPT) on short rainbow stacks throughout the project of typical duration of 1800 hours each [4]. Among them, the third series of LPT (LPT3) was selected

for the creation of FPT's final version of degradation model[1]. Starting from LPT3 and on, Bosch employed the testing protocol developed by themselves using FPT's stack load profile data.

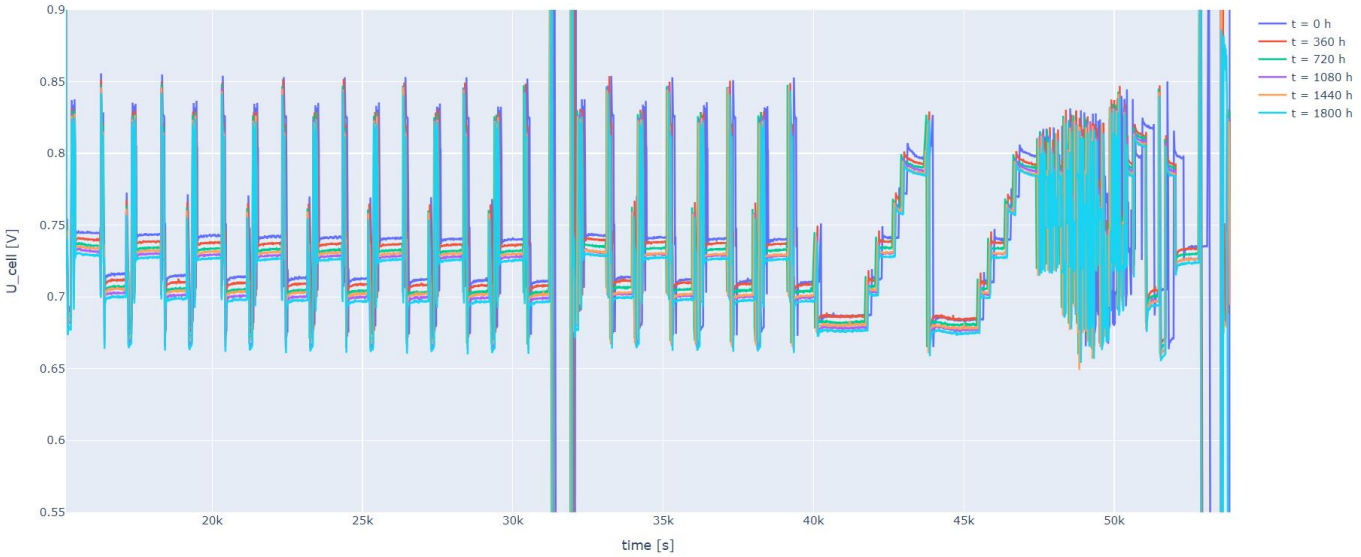

Figure 1. Average cell voltage vs. time every 360 hours from the beginning of testing. LPT3 data for the baseline fuel cells.

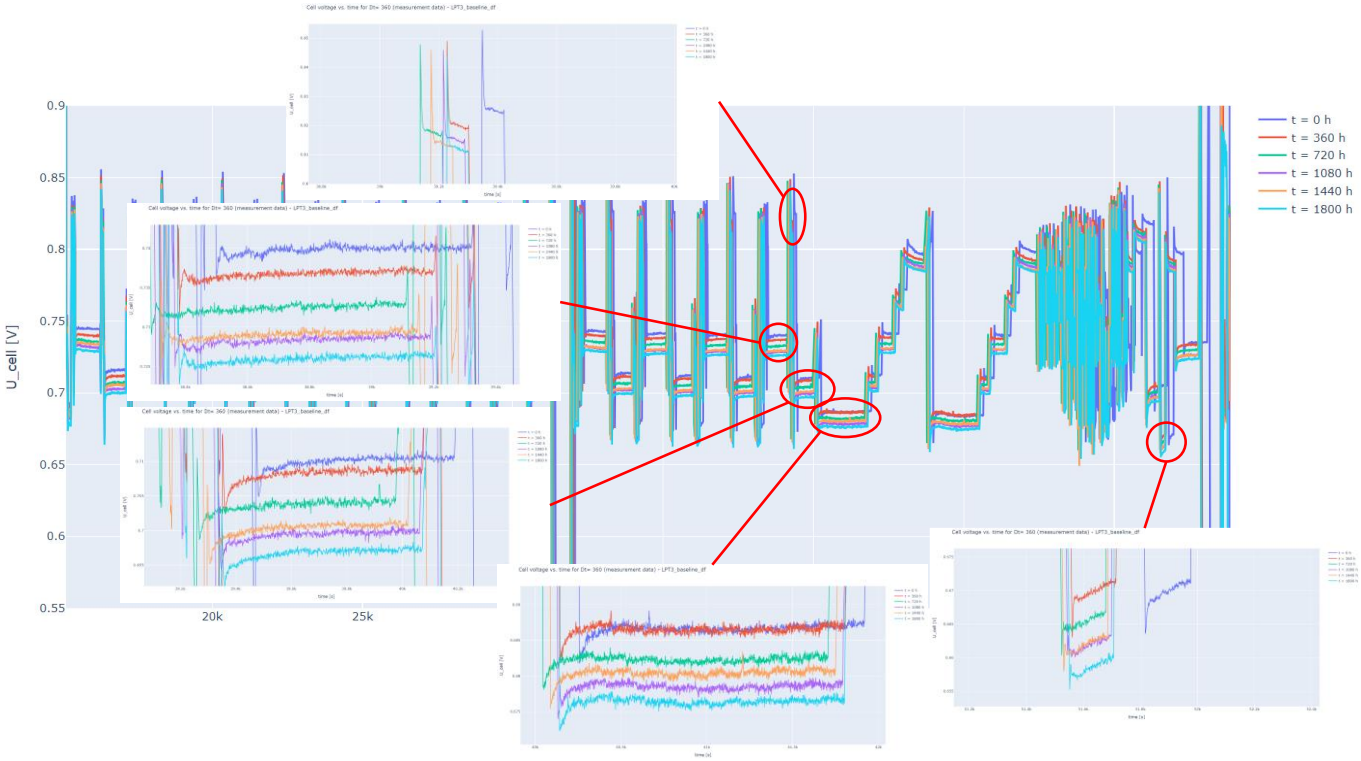

Figure 2. Zoom in Figure 1 depicting degradation of average cell voltage at various voltage levels. LPT3 data for the baseline fuel cells.

Figure 1 depicts experimental data (average cell voltage) based on LPT3 at different testing times, starting from t = 0 up to t = 1800 h with 360 h (15 days) time intervals. Figure 2 zooms in at various voltage levels,

[1] Earlier modelling approaches using LPT1 measurements are not discussed here.

showing the evolution of degradation in more detail. The sampling times resolution is 1 s (1 Hz), resulting in about 6.5 million data points. Each measurement point includes stack and cell voltages, current (set and real values), pressures, temperatures, humidity, flowrates etc. Figure 3 depicts the evolution of the average cell voltage for the entire LPT3. Degradation can be distinguished, although less clearly.

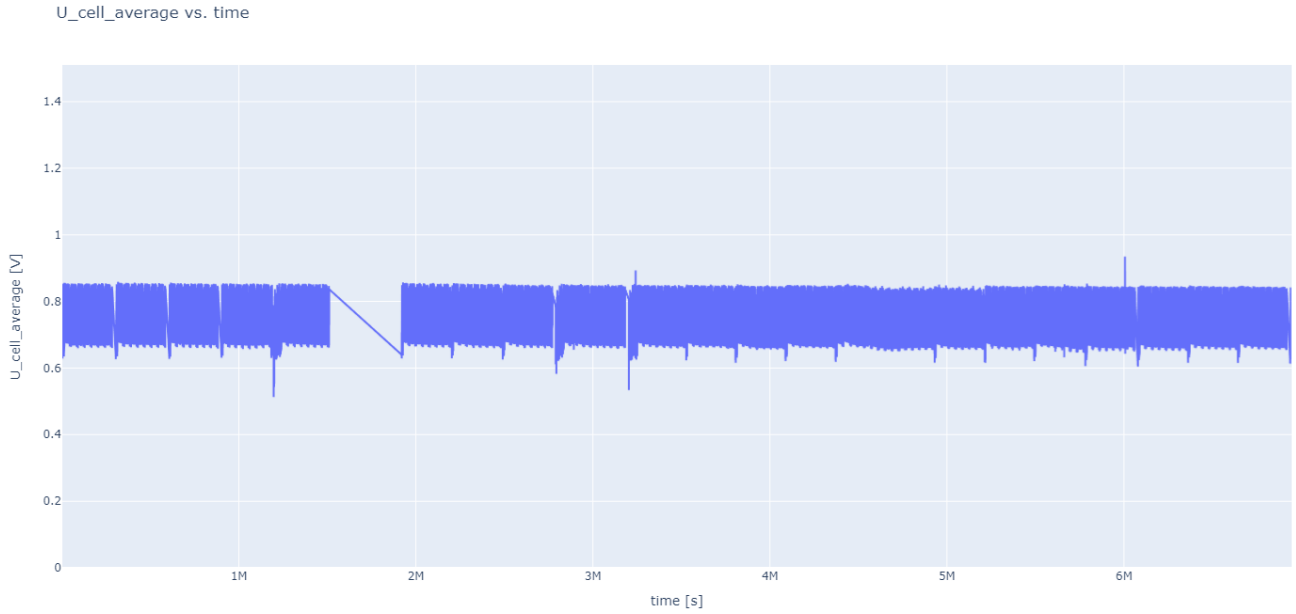

Figure 3. Evolution of the average cell voltage of the baseline stack for the entire LPT3. The gap between t=1.5 Ms and t = 1.85 Ms is probably due to an artefact in the data export. There was no shutdown and no influence on the subsequent calculations.

2.1.2 "Shallow" neural network and features creation

For fast calibration and running times as well as easier integration to future models that are often developed in platforms such as MATLAB™ and Simulink™, or even Excel, a linear modelling approach was selected. Moreover, in the development of statistical models it is generally a good practice to start from simple approaches and revert to more complex machine learning techniques in case the simpler approaches are not satisfactory.

Among the available input data for the linear model after a first pre-processing phase, effectuated during the development of the first models with LPT1 data, several measurements were excluded as predictors (independent) variables because of their high correlation, which would not add value to the model and would induce high multicollinearity [5]. In the end a total of eight measured (8) predictors were used as input (Figure 4) including current density, pressure, temperature, humidity, and flowrates. Starting from the eight inputs, a series of features was created from the basic predictors[2] ($[\phi_X]_i$ in Figure 4), which, multiplied by respective constants (weights) and added as terms of a linear model provide the model output. Among the introduced features, the current density dynamic throughput as defined in the Appendix A (§6, p. 35) and two features accounting for the dynamic behaviour of the stack were included.

This approach, which is schematically depicted in Figure 4 recalls the operation of neural networks with the eight measured predictors being the input layer and the features stemming from the basic predictors

[2] Features being essentially functions of the inputs. This process is also called "feature engineering".

This project has received funding from the Fuel Cells and Hydrogen 2 Joint Undertaking (now Clean Hydrogen Partnership) under grant agreement No 101006641. This Joint Undertaking receives support from the European Union's Horizon 2020 Research and Innovation programme, Hydrogen Europe and Hydrogen Europe Research.

being the hidden layer. Thus, the term "shallow neural network" or "shallow learning" is sometimes used alternatively.

In the entire modelling campaign, where several models were tried, the number of terms varied, typically from 77 up to 173 terms. The final selected model had 93 terms.

The output of the model is the average cell voltage of all baseline cells used in the rainbow stack. The model was calibrated for current density in the range 0.08 – 1.50 A/cm^2, under the assumption that values beyond that region would be of no practical use for the purpose of the model (fuel cell vehicle simulation for WP6 deliverables D6.3 and D6.4 [1]). Furthermore, with this approach strong non-linear behaviours of the stack, which would make the modelling process even more challenging, were also avoided.

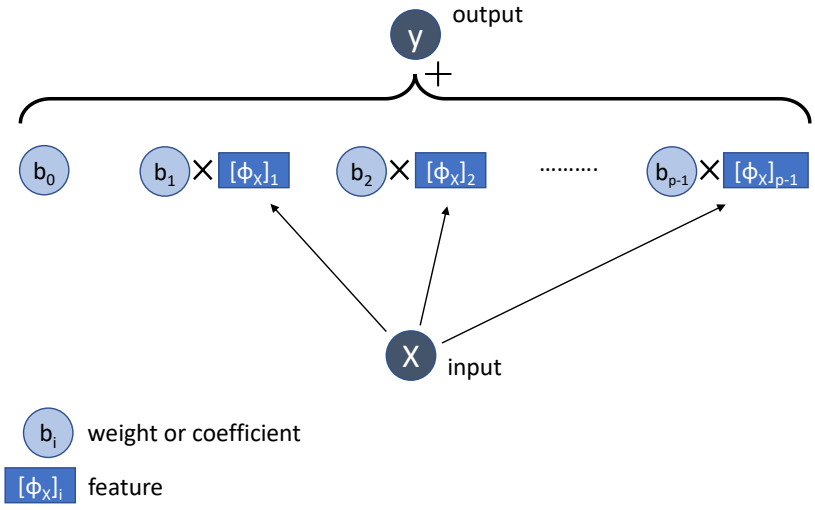

Figure 4. Linear model or "shallow" neural network. X is the array of inputs. The features φ are functions of elements of X. (schematic inspired by [6]). The number of terms (features or predictor variables) is p.

Dynamic throughput as predictor of degradation

Since the scope of the produced model is the forecasting of the fuel cell stack's degradation as a function of its operation conditions, relevant stressors needed to be included. Typical stressors for degradation are the operating conditions already included in the model input (temperature, humidity, pressure) as well as the usage of the fuel cell. One metric that is often used for the latter, especially within the context of integrators' industry, is the time of operation. However, this is not accounting for the real operating conditions and was therefore rejected as factor in the model[3]. Alternatively, the current density throughput and its dynamic throughput were considered (Appendix A). During the development of the various models, they were both very highly correlated, and inclusion of both in the model would lead to unsuccessful models. Given that it is well-known that the operation dynamics have an impact on the fuel cell's durability, the dynamic throughput was finally used.

The impact of start-up and shutdowns, related to the air front at the anode, was not considered in this model.

[3] There have been attempts to include time in early experimentations, but they were finally rejected.

2.1.3 Sub-sampling and robustness of statistical model

One issue that may arise when developing models with many factors, is a potentially high multicollinearity [5]. While collinearity of factors is unavoidable in complex models, what is important is that:

a) the regression method retains its capability to calculate the coefficients (weights) of the model[4], and
b) the model remains robust to small variations either of the input or the coefficients,

Furthermore, it is desired that the model is immune to outliers as much as possible.

A method to address all the above points and render the model more robust, is the creation of multiple models with the use of re- and sub-sampling [7], and this is what was applied in this case too. Figure 5, depicts the steps that were followed for the calculation of the model's calculation. Firstly, the data set was split randomly to train and test data. 70% of the train data were randomly reshuffled 101 times and they were used each time to calculate the model's coefficient. The final set of coefficients was the average of the 101 sets, while the original test data (20% of the original data) were used for model validation. An example of such validation with test data is shown in Figure 8 (histogram).

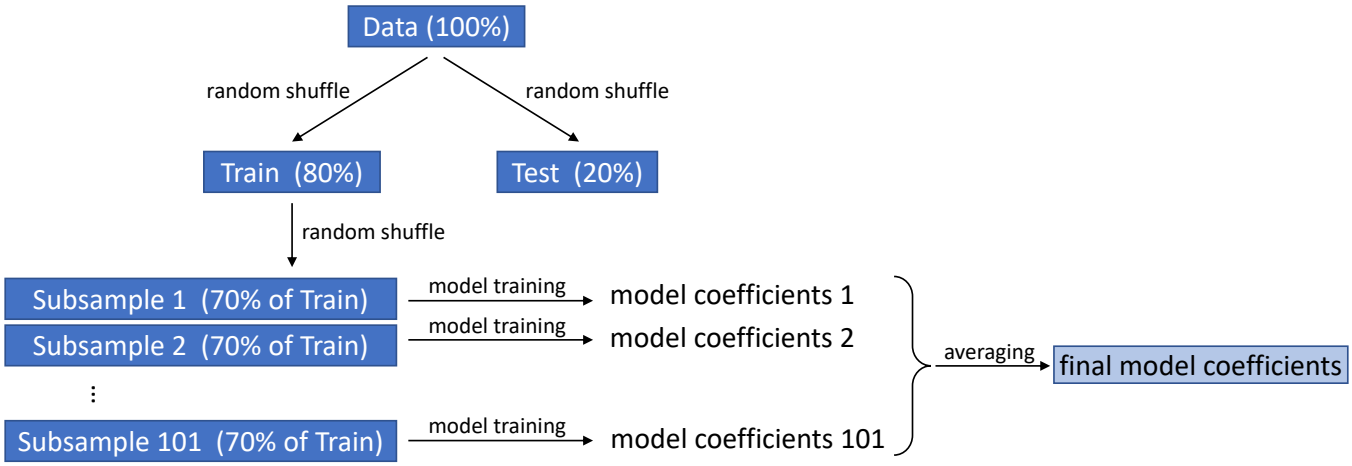

Figure 5. Sub- and re-sampling of data. The initial data were split randomly to Train (80%) and Test (20%) data sets. The Train data were not used in their entirety for the model calibration. 70% of them was randomly selected and used to train the model. This was done 101 times, producing 101 different sets of coefficients. The 101 coefficients were averaged to produce the final set of the model coefficients. The Test data are used to validate the model.

2.1.4 Calculation of uncertainty / confidence interval

An important advantage of linear models is the existence of relatively straightforward formulas that help calculate the uncertainty of the prediction of the model. This applies to multi-dimensional models as well as one-dimensional models. The reader is referred to good textbooks in linear regression such as [8] for the relevant background. The formula used in this application for the calculation of the variance of the value predicted from the model is the following:

$$s^2\{prediction\} = MSE_{train}\frac{h_h}{\bar{h}}[1 + h_h] \quad (2.1)$$

[4] Collinearity reduces the capability of the modelling solver to solve ordinary least squares equations and may result to erroneous calculations of the coefficients.

This project has received funding from the Fuel Cells and Hydrogen 2 Joint Undertaking (now Clean Hydrogen Partnership) under grant agreement No 101006641. This Joint Undertaking receives support from the European Union's Horizon 2020 Research and Innovation programme, Hydrogen Europe and Hydrogen Europe Research.

where:

- $s^2\{prediction\}$ is the variance of the model predicted value.
- $MSE_{train}$is the mean squared error from the model training[5]
- h_h is the "hat" value of the predicted new data point.
- $\bar{h}$ is the average "hat value" of the data points used for the model training

"Hat values" are described and explained in the Appendix B (§7, p.36).

NOTE: This equation is an adaptation of the original equation given in [8]. The rationale for this adaptation is expressed in the Appendix B, were further explanations and definitions are provided.

Once the variance is calculated for each predicted point, it's 95% confidence interval can be estimated as:

$$\pm 2s^2 \cdot \{prediction\} \tag{2.2}$$

2.2 Selection criteria for forecasting model selection

As mentioned in §2.1.2, many models were tried until a satisfactory was chosen, a linear model with p=93 coefficients, or 92 predictor features plus a constant. When there are many models available, relevant criteria must be set for the final selection. In the current work attention was drawn to the following:

- How well the model fits the available data
- How well the model extrapolates from a part of the data to the entire available data set
- What is the precision when the model extrapolates beyond the measured horizon.

The next paragraphs elaborate on the above three criteria.

2.2.1 Fitting to the training and test data

Model fitting can be assessed with many different criteria. Typical and very intuitive is the direct graphical comparison between measurements and model output, such as the one shown in Figure 6 with the time evolution of the average cell voltage, where a good fitting is demonstrated, mainly in the less dynamic conditions. Alternatively, the voltage versus the current density can be juxtaposed as is done in Figure 7. In both cases, the difference between data and model (residual) can be assessed qualitatively and marginally quantitatively.

[5] In this application the MSE from the test data was used, which essentially was equal to the training MSE

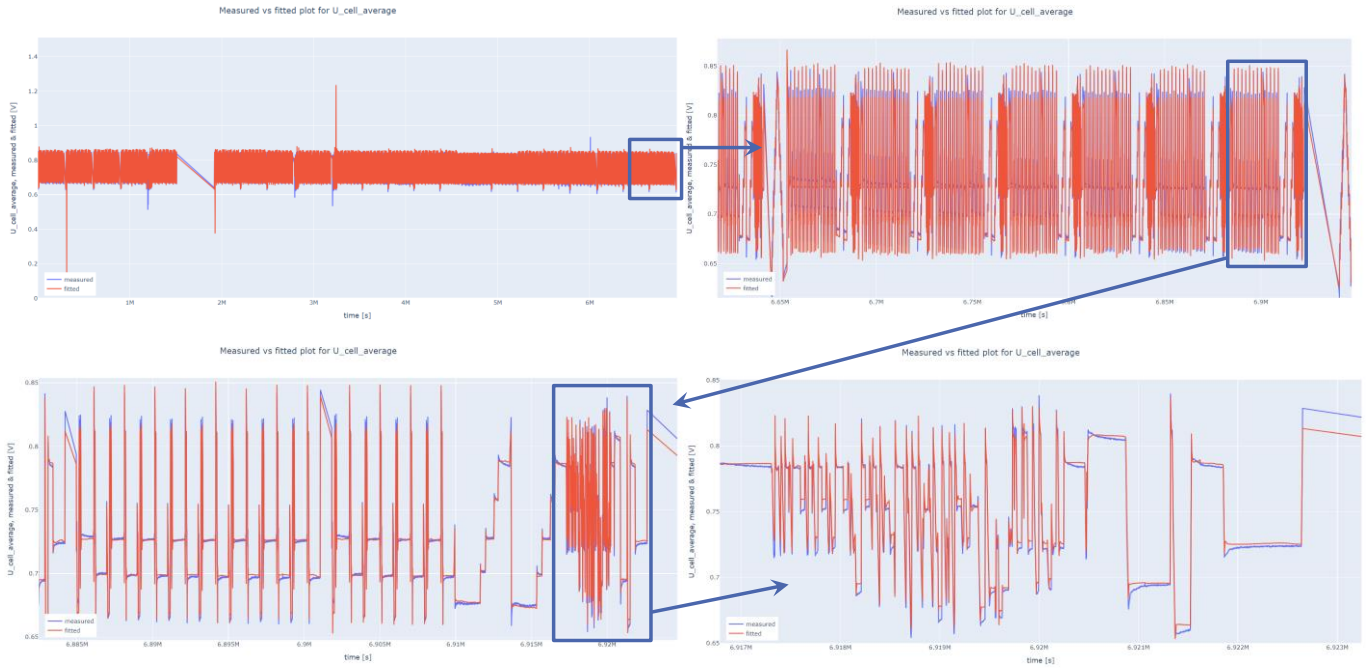

Figure 6. Overview of model fitting in time series with consecutive zooming-in.

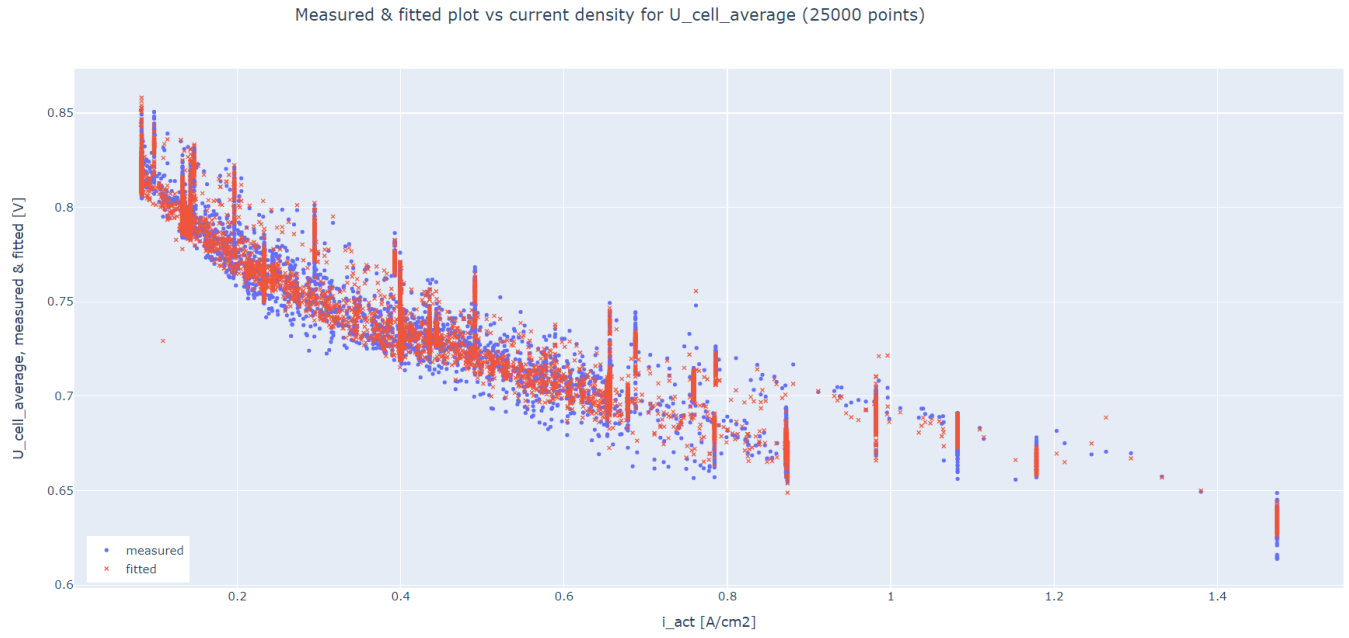

Figure 7. Average cell voltage vs. current density. Due to the large amount of data, only a random selection of 25000 data points is shown.

A histogram of the residuals, such as the one depicted in Figure 8, is a more precise quantitative assessment of the fitting giving a different perspective of the spread of the model's deviation. It is noteworthy that the histogram of Figure 8 is showing fit to the test data, i.e., the data reserved for model validation and not the ones used for training.

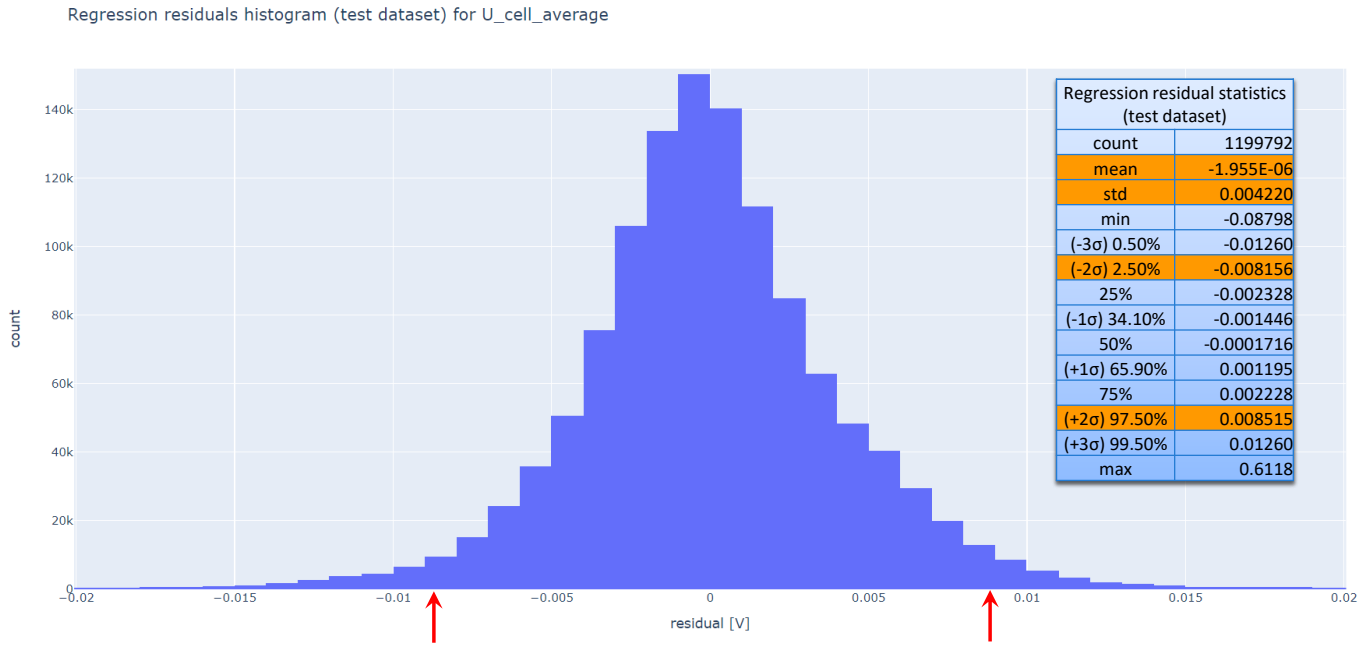

Figure 8. Regression residuals histogram for the test data set (i.e., validation data set) and table with main fitting statistics. The red arrows are showing the ±2σ (95%) confidence interval.

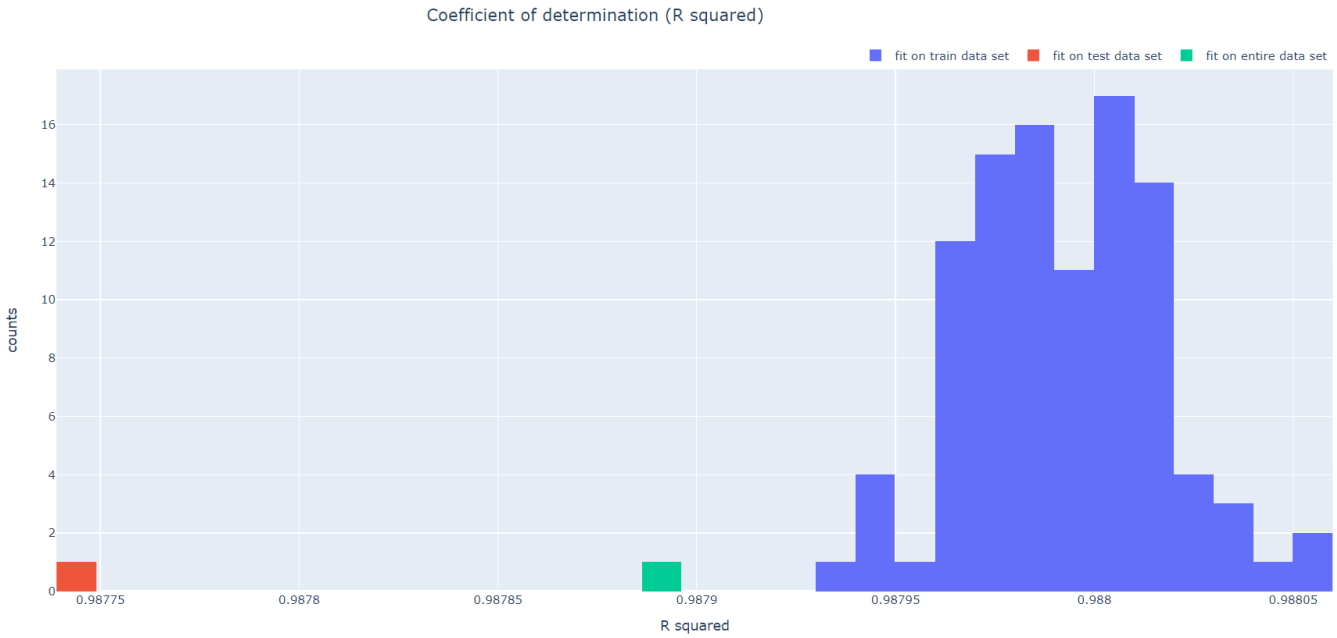

Figure 9. Coefficient of determination (R^2) of the model, for the 101 train data sets (blue, right), the test (red, left) and the entire data set (green, middle).

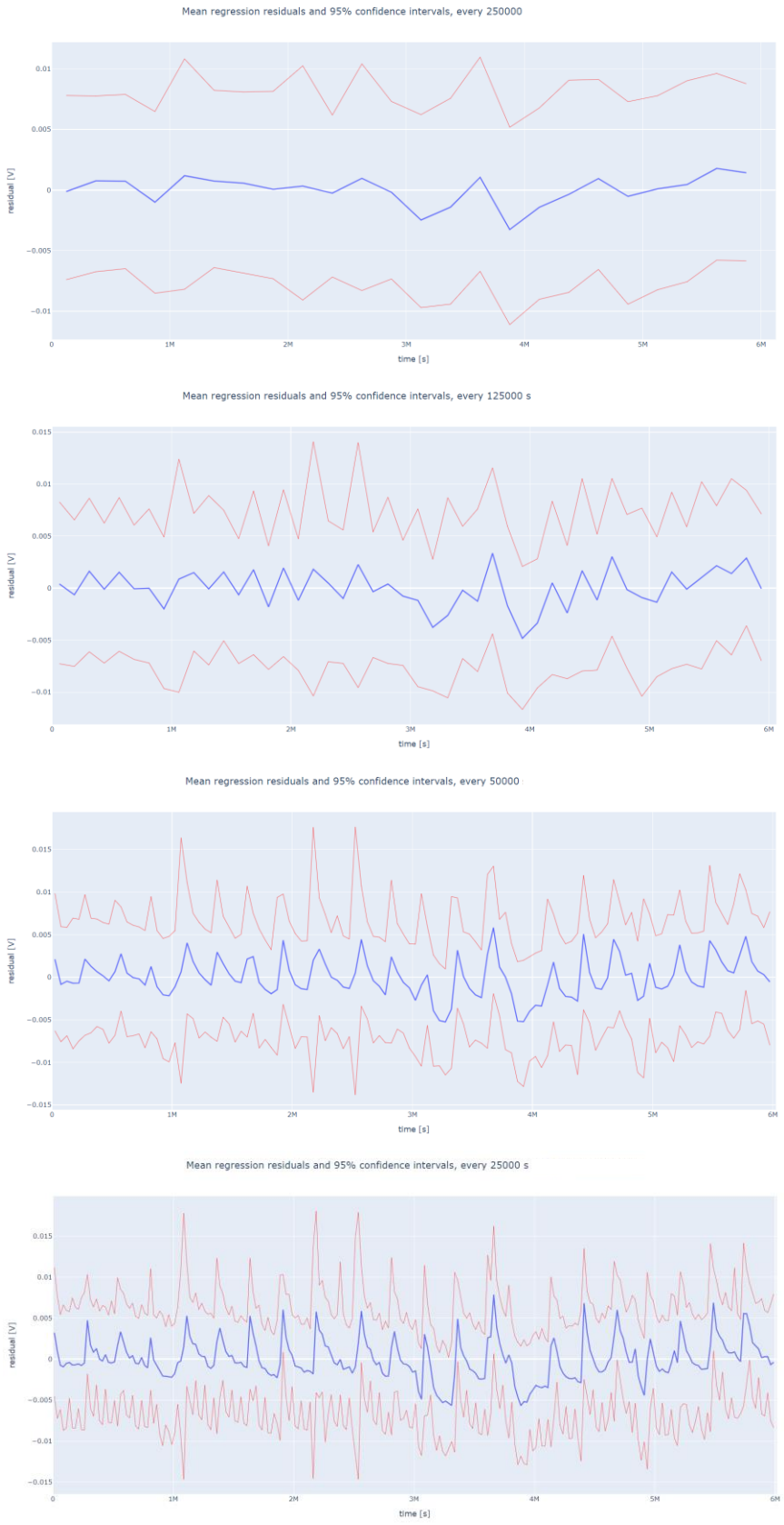

Figure 10. Mean error and 95% confidence trends for various data batches.

This project has received funding from the Fuel Cells and Hydrogen 2 Joint Undertaking (now Clean Hydrogen Partnership) under grant agreement No 101006641. This Joint Undertaking receives support from the European Union's Horizon 2020 Research and Innovation programme, Hydrogen Europe and Hydrogen Europe Research.

Figure 8 is also showing that the distribution of the error is not a normal (Gaussian) distribution, rather it seems to be a Laplace or another distribution from the symmetric exponential family[6,7]. The same Figure is providing a table with the main statistics. What is noteworthy is that because the distribution is not normal, the 31.8% error does not correspond to ±1σ (±one standard deviation), but much less, while the 95% and 99% errors do correspond to ±2σ and ±3σ respectively. The very thin and long tails apparently represent the deviations in the fuel cell dynamics.

In some cases, the coefficient of determination – also known as "R-squared", expressing the fraction of the data that are explained by the model − is a metric of interest. Figure 9 presents a histogram with the R^2 values for all fitted cases, that is, the 101 train data sets, the validation test data, and the entire data set. Even in the worst case, the test data value has an R^2 of about 0.988.

2.2.1.1 Residual trends

An important qualitative technique to test the fit of a model is to observe the evolution of the residual over time. This way any trends, such as increases or decreases in time, or patterns, such as cyclic behaviours, may be quickly perceived. In a good fit, there should be no correlation between time and residuals and the error should look random.

Given that the amount of data is so large that such a graph would be too confusing, the trend was examined in batches of 25000, 50000, 125000 and 250000 data points, where the arithmetic mean of the error for each batch is plotted. Figure 10 is showing a series of graphs with the residual trends of the selected regression model. When the batches are large, no trend is shown, rather the error, leading to the conclusion that asymptotically the model is not influenced by any seasonality. However, when the sampling is refined, especially for 50000 and 25000 data points, the errors are periodic, with a high peak of about 5 mV, a little higher than the standard deviation is repeated. This means that there is a subset of the data where the model is not as successful as for the rest.

2.2.1.2 Forecasting of degradation

An interesting check that can be done is how well the model fits degradation specifically. This is examined in the table of Figure 11, which is comparing the voltage drop (in Volts) from t=0 to t=1800 in the real baseline stack and for a selection of five models, and current densities. The models are generally underestimating degradation. One reason for this may be that even degradation seems to have a stochastic behaviour, and it is not monotonically increasing, as can be clearly seen in the inset pictures of Figure 2.

Emphasis is mainly given to the three last columns of the table, that correspond to current densities higher than 0.65 A/cm^2, and that have more practical value for a fuel cell truck application. It is repeated here that the model was trained in the region 0.08 – 1.5 A/cm^2, and therefore the first two columns should not be expected to have as a good fit.

The selected model is #2 in the table and Figure 12 is showing how it is replicating Figure 11, and forecasts degradation. The operating conditions that were assumed in the simulation are described in §2.3.

[6] No statistical test was performed for confirmation of the assertion or the calculation of the distribution parameters.
[7] If this is the case, then the result of least squares is not providing the maximum likelihood estimator; the minimum sum of absolute errors (L-1 distance) should be used instead.

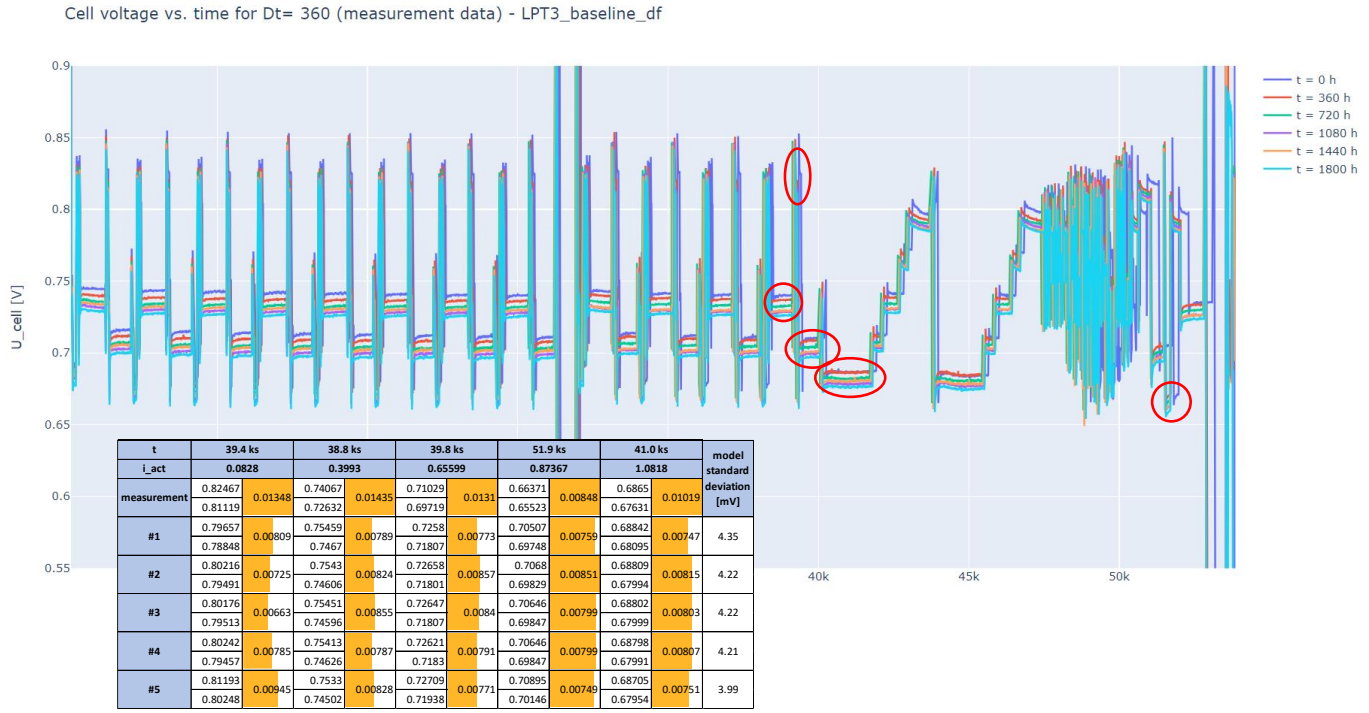

t	39.4 ks		38.8 ks		39.8 ks		51.9 ks		41.0 ks		model standard deviation [mV]
i_act	0.0828		0.3993		0.65599		0.87367		1.0818		
measurement	0.82467	0.01348	0.74067	0.01435	0.71029	0.0131	0.66371	0.00848	0.6865	0.01019	
	0.81119		0.72632		0.69719		0.65523		0.67631		
#1	0.79657	0.00809	0.75459	0.00789	0.7258	0.00773	0.70507	0.00759	0.68842	0.00747	4.35
	0.78848		0.7467		0.71807		0.69748		0.68095		
#2	0.80216	0.00725	0.7543	0.00824	0.72658	0.00857	0.7068	0.00851	0.68809	0.00815	4.22
	0.79491		0.74606		0.71801		0.69829		0.67994		
#3	0.80176	0.00663	0.75451	0.00855	0.72647	0.0084	0.70646	0.00799	0.68802	0.00803	4.22
	0.79513		0.74596		0.71807		0.69847		0.67999		
#4	0.80242	0.00785	0.75413	0.00787	0.72621	0.00791	0.70646	0.00799	0.68798	0.00807	4.21
	0.79457		0.74626		0.7183		0.69847		0.67991		
#5	0.81193	0.00945	0.7533	0.00828	0.72709	0.00771	0.70895	0.00749	0.68705	0.00751	3.99
	0.80248		0.74502		0.71938		0.70146		0.67954		

Figure 11. Fitting of various models on degradation trends. The table is showing the voltage drop in Volts at various current density levels (see also Figure 2) from t=0 to t=1800 h. The selected model is #2.

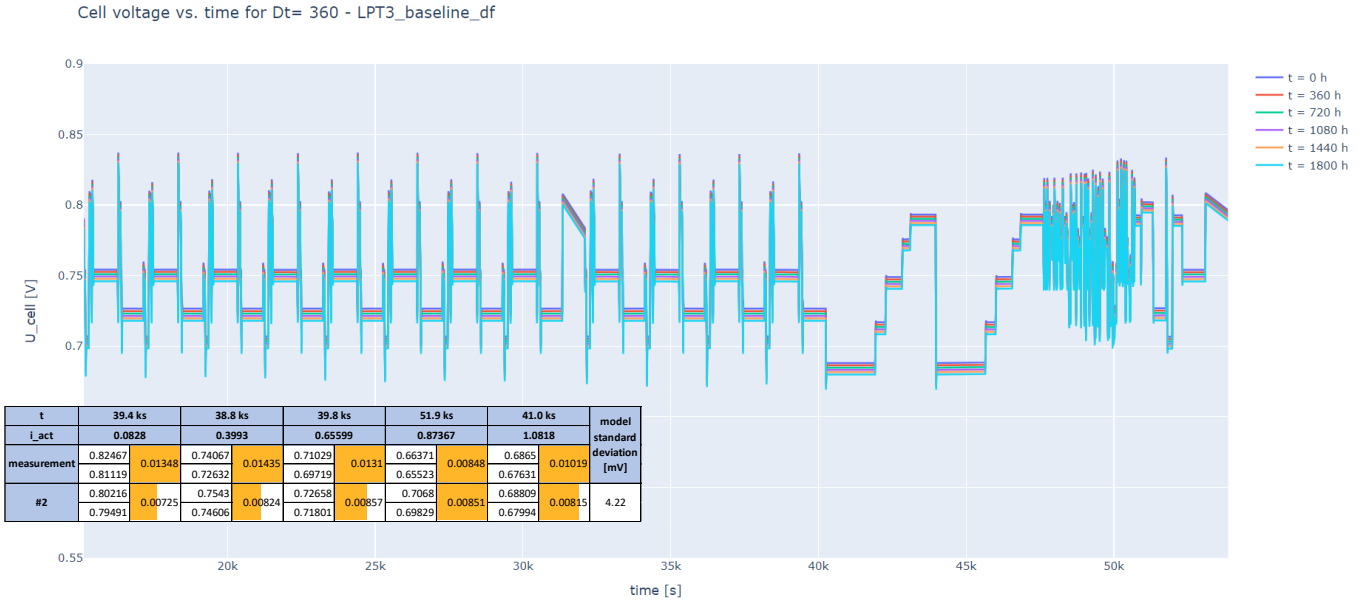

t	39.4 ks		38.8 ks		39.8 ks		51.9 ks		41.0 ks		model standard deviation [mV]
i_act	0.0828		0.3993		0.65599		0.87367		1.0818		
measurement	0.82467	0.01348	0.74067	0.01435	0.71029	0.0131	0.66371	0.00848	0.6865	0.01019	
	0.81119		0.72632		0.69719		0.65523		0.67631		
#2	0.80216	0.00725	0.7543	0.00824	0.72658	0.00857	0.7068	0.00851	0.68809	0.00815	4.22
	0.79491		0.74606		0.71801		0.69829		0.67994		

Figure 12. Degradation forecasting by the model #2 (see also Figure 11). The operating conditions as defined in §2.3 (Figure 15) were used.

2.2.2 Behaviour in extrapolation from partial to full data

Once the fit of the model is assessed, using appropriate criteria from the statistics literature, a forecasting model needs to be tested as to whether it can forecast the data trends. In the current work, this was done by training on part of the available data and then observing how the fit evolves for the rest towards the future.

Figure 13 is depicting models that were trained with data of about 900 hours and then let extrapolate up to the end of testing. During training all of them had similarly good fitting behaviour. However, extrapolation beyond the training area would lead to unacceptable deviations.

The case at the bottom right of Figure 13, emphasised with a red frame, corresponds to the selected model.

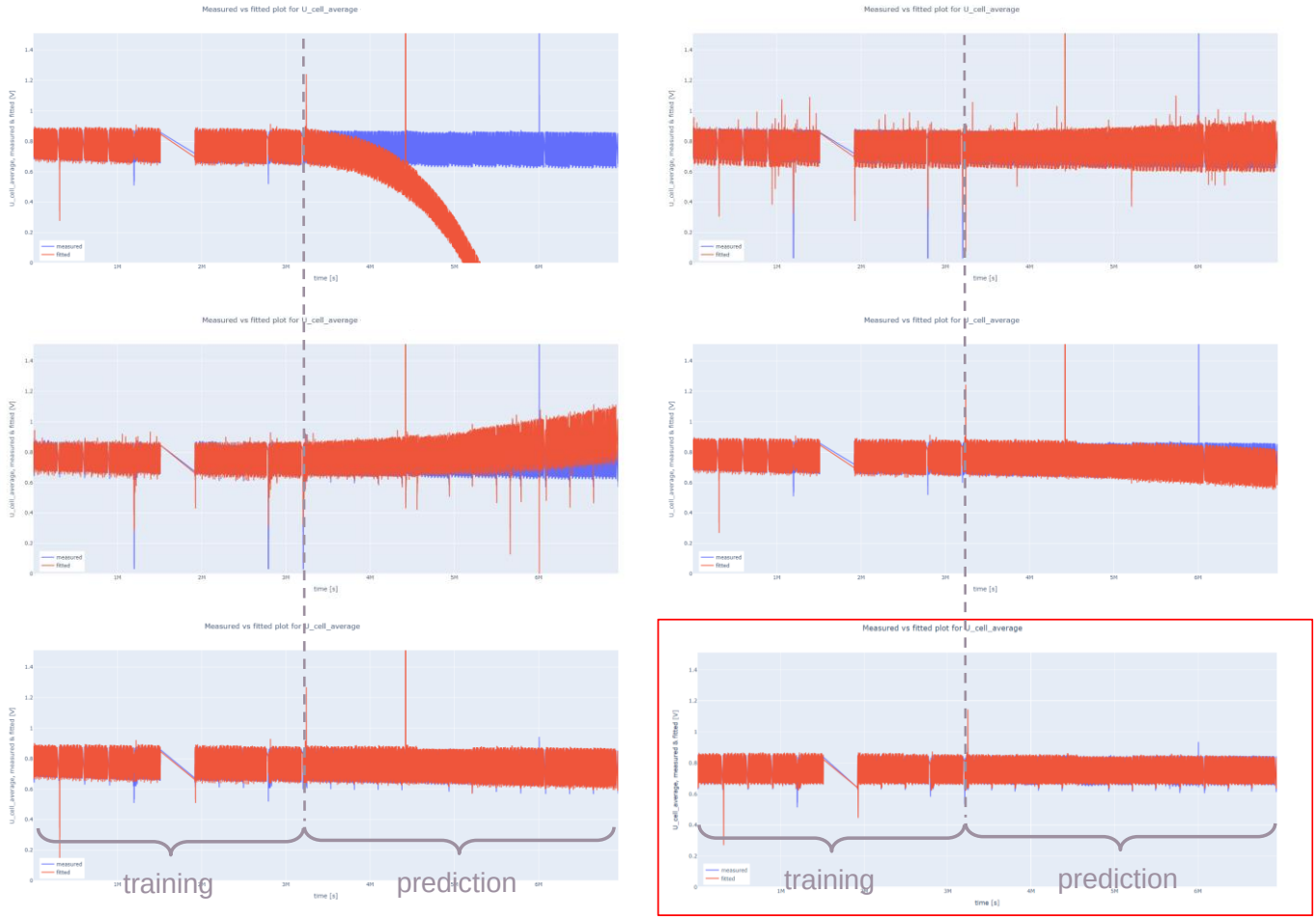

Figure 13. Extrapolation from partial training. Among the 6 different models, the one at the bottom right has the best forecasting behaviour. All models had similar fitting precision on the test data during training.

2.2.3 Precision in extrapolation to the future

The last criterion for model selection that was established in this work was to assess how the model extrapolates beyond the end of testing, in the future. Since there are no relevant data to compare, the assessment was done on the precision of the model as measured with the confidence interval of the forecasting. A model with narrower confidence interval is preferrable.

In Appendix B it is explained that the prediction error depends on the "hat values" of the predicted outputs, and they are changing with every model. This is demonstrated in Figure 16. In this Figure, the output of four different models – the numbers correspond to the ones in the table of Figure 11 – for times t=0 and t=30000 h along with their confidence intervals are juxtaposed. While at t=0, the prediction errors are very similar, the ones for the extrapolation to the far future vary considerably. It is also notable that

the error is changing for different voltage levels, given that the corresponding points have different "distances" (hat values) from the train data centroid.

The selected model #2 is on the top right corner in red frame. A 20% degradation (136 mV) is forecast at the maximum 1.08 A/cm^2 after 30000 hours.

Figure 14. Confidence intervals of voltage forecasting in LPT1 at t=0 and t=30000 h, for four models of the table in Figure 11.

2.3 Operating conditions and behaviour of the model at different load profiles

Once the candidate regression models have been assessed and one among them is selected according to the criteria of §2.2, and before its use in different missions one more step needs to be taken. Although the model is flexible enough to have different operating conditions as input (pressures, flowrates, temperatures, and relative humidity, it is preferable to determine the operating conditions as a function of the current density, simplifying this way future applications.

For the selected model this was done by using the operating conditions at the test bench as reference, under the assumption that these conditions are the most appropriate, if not optimised, for the specific cell. Figure 15 is showing how the operating conditions are correlated – to one degree or another – to the current density. The yellow line depicts the sought function that was finally defined. The same function was used to produce the result of Figure 12.

After the definition of the operating conditions, the model was used to simulate the baseline cell's output for the four load profiles that were shared with the IMMORTAL project partners at the end of the first year of the project [1]. The simulation was done for t=0 as well as t=30000 hours. The results are depicted in Figure 16 and they show varied cell degradation as well as confidence intervals. For example, run #197, which is much smoother than the other three, degrades the cell comparatively little while the uncertainty is quite higher. Apparently, the operating points extrapolated to 30000 hours deviate from the centroid of the training data much more than for the other cases. Run #241 has the narrowest confidence interval. As in the cases of Figure 14, the uncertainty is changing with the current density.

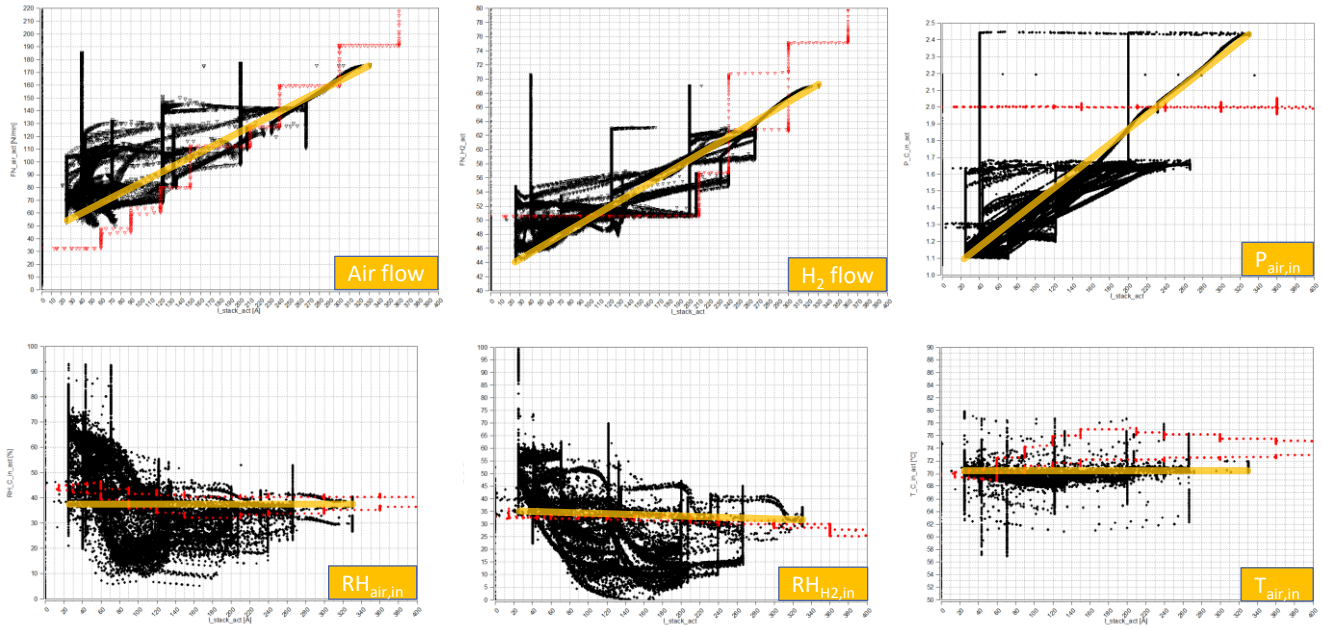

Figure 15. Determination of inputs for the regression model. Black: mission data, red: polarisation curve data. The yellow lines are the defined model inputs as functions of the current density.

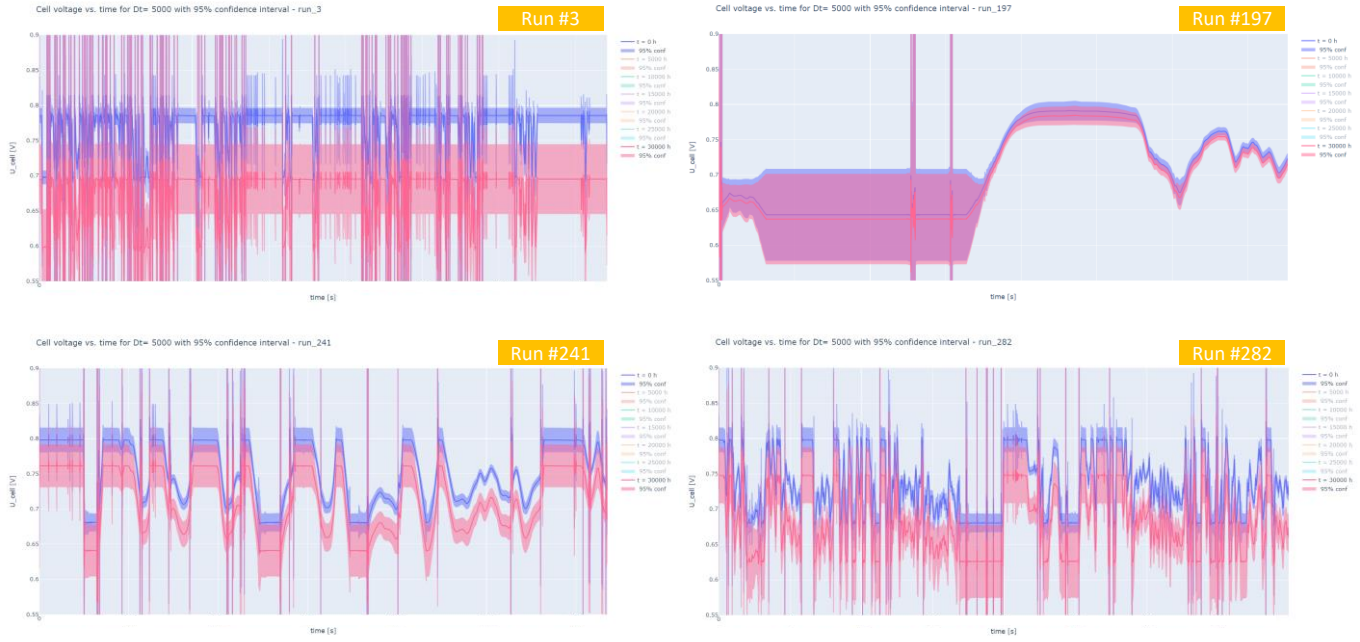

Figure 16. Voltage forecasting at t=0 and t=30000 h of the selected final model for simulation runs #3, #197, #241 and #252.

3 AN ALTERNATIVE APPROACH FOR LOAD PROFILE CREATION FOR DURABILITY TESTING

3.1 The importance of experimental data quality for the creation of statistical models and the extraction of information in general

It is well known that good data quality is of determining importance for any statistical work, including statistical inference and modelling for behaviour forecasting. This is the reason that the methodologies of Experimental Design have been developed and extended literature has been published (e.g., [9]).

This applies to the creation of models for this work's application too. Figure 17 depicts the two different testing protocols applied for LPT1 & 2 and for LPT3 & 4. On the left and top are the initial load profiles, based on "sweeping" of the current density at a specific frequency with differentiation only on the low voltage level (LL – red circles) and the hold time at high voltage (green circles) [1]. At the bottom right of the same figure, the new protocol is shown, based on simplification of the load profiles #3, #197, #241 and #282 (Figure 16) [4].

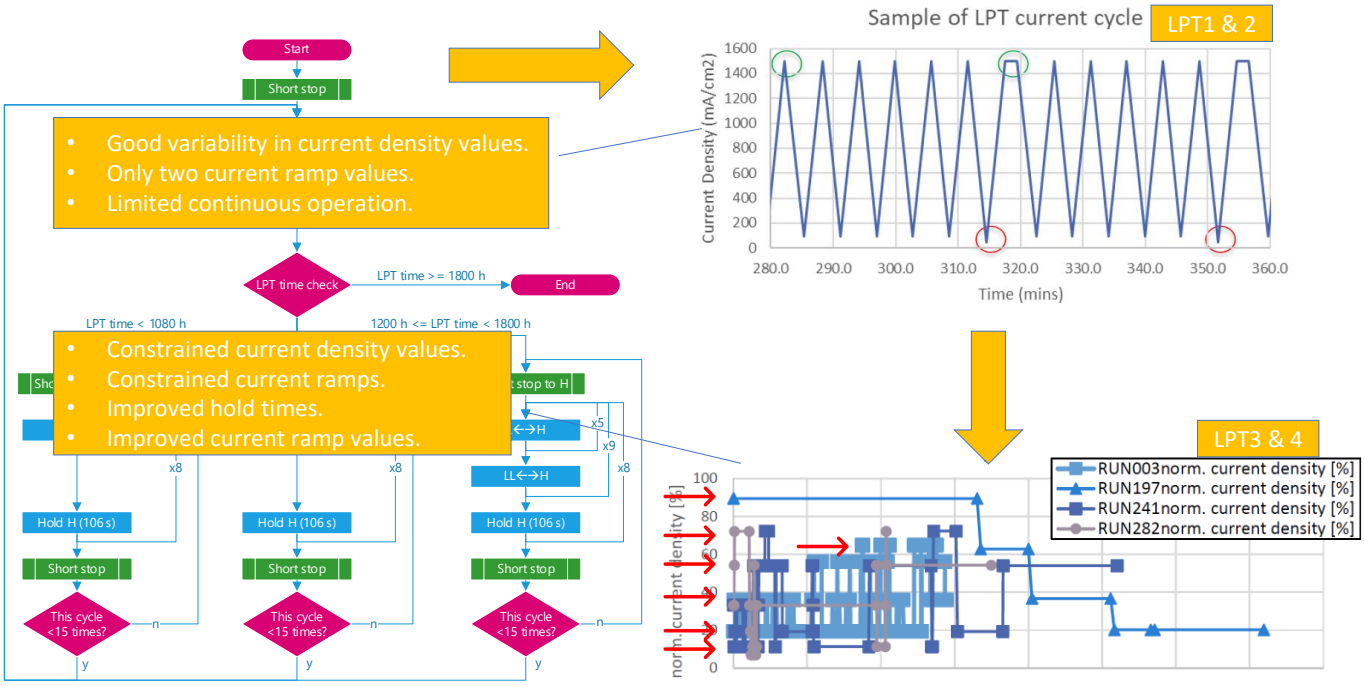

Figure 17. Two different testing protocols producing data of different quality ([1] & [4]).

Both LPT approaches have their pros and cons. LPT1 & 2 present good variability in the current density, due to the current "sweeping". However, the current ramps have only two values, and those are very close to each other, which does not allow better understanding of the impact of current slope on the fuel cell behaviour and durability. Furthermore, the hold times are very limited. On the other hand, LPT3 & 4, which are based on real-life data have improved hold times and current ramps, while, due to their processing and simplification the current values are constrained at specific levels, the ones shown in red arrows.

Yet, when developing a model, variability in the data is necessary in order to:

- Reduce correlations between factors, i.e., the correlations between the model coefficients.

- Broaden the range of application for the model, that is when the spectrum of the data is broad, the model's capability to extrapolate improves.
- Increase the possibility to try different modelling approaches.

This applies to any type of model, physical, empirical or semi-empirical, other mathematical approach or even in look-up-tables (LUT) form. Sometimes the form of the data set may be restrictive for specific types of models. This was the case for the first models created based on LPT1 data. They could not be calibrated with the LPT3 data and new needed to be created.

Given this experience, the general knowledge of the relation between data quality and modelling, as well as the observation on how fuel cell scientists are developing LPT (load profile tests) and ASTs (accelerated stress tests), which are also very limited, the author is proposing in this section a different approach, where randomisation is "injected" into the characteristics of an LPT, in a way that the new LPT that is created has a broader spectrum of value while maintaining features that the designer of the experiment desires. This is done with the use of Markov chains, which are memory-less stochastic processes.

Furthermore, given that the new LPT that is produced with the proposed method is stressing the fuel cell considerably more than its normal use, it can be considered an Accelerated Durability Test (ADT[8]). This is the term that will be used from this point on.

3.2 Markov chain-based Accelerated Durability Testing (MCADT)

3.2.1 Principles

It is out of scope to present Markov chains here. A first understanding can be obtained on the relevant Wikipedia lemma [11] or other Web pages found on the Internet. It is only mentioned that a Markov chain is a discrete stochastic process[9] where the state of a system – in this case the current density of a fuel cell – at discrete time intervals is a random variable, determined in a matrix defining the probability of transitioning to the next value given the previous value.

This can be better understood by the example of Table 1 showing such a transition matrix. By knowing the current density value at time t_i, say 0.7 A/cm^2, the probability to transition to another current density level at the next time instance t_{i+1} is given by the elements of the row that corresponds to the "before" value. In the example, the probability that the fuel cell will have current density 0.8 A/cm^2 at t_{i+1} is 10%, while the probability that it will remain 0.7 A/cm^2 is 75%. The sum of probabilities for each row must be 100%.

Once the transition matrix is defined, a stochastic process may be created with the use or random number generator. Figure 18 and Figure 19 are presenting such examples.

It is up to the experimenter to define the desired transition times $\Delta t = t_{i+1} - t_i$. In the examples here, $\Delta t = 1s$ was chosen, equal to the time resolution of the LPT data of §2.1.1 (p. 5). With the Δt known, desired average hold times may be determined especially if specific load profiles need to be approximated, according to the following formula, upon which Table 2 is based.

[8] The author encountered the term in the conference presentation [10] for the first time.
[9] There are also continuous Markov chains which do not relate here.

$$transition\ probability = 1 - \frac{transition\ time}{mean\ residence\ time} \tag{3.1}$$

Indeed, from the diagonal of the transition matrix (Table 1) one can see that the average hold time for 0.6 A/cm^2 is 50 s, that can be seen in the graphs of Figure 18 and Figure 19.

Finally, the current slopes can be configured like the hold times. Table 3 shows that the relative frequencies for slopes ±0.1 A/cm^2/s and ±0.2 A/cm^2/s, i.e., the relative probabilities for all transitions except the diagonal are set to specific values. Their sum is 90%, giving a 10% margin for other transitions to take place with equal probability.

Table 1. Transition matrix for the creation of a stochastic process defining the load profile of a fuel cell.

current density before \ current density after	0	0.1	0.2	0.3	0.4	0.5	0.6	0.7	0.8	0.9	1	1.1	1.2	1.3	1.4	1.5	1.6	1.7	1.8
0	0.80000	0.08000	0.03000	0.00563	0.00563	0.00563	0.00563	0.00563	0.00563	0.00563	0.00563	0.00563	0.00563	0.00563	0.00563	0.00563	0.00563	0.00563	0.00563
0.1	0.06250	0.75000	0.10000	0.03750	0.00333	0.00333	0.00333	0.00333	0.00333	0.00333	0.00333	0.00333	0.00333	0.00333	0.00333	0.00333	0.00333	0.00333	0.00333
0.2	0.02500	0.06250	0.75000	0.10000	0.03750	0.00179	0.00179	0.00179	0.00179	0.00179	0.00179	0.00179	0.00179	0.00179	0.00179	0.00179	0.00179	0.00179	0.00179
0.3	0.00179	0.02500	0.06250	0.75000	0.10000	0.03750	0.00179	0.00179	0.00179	0.00179	0.00179	0.00179	0.00179	0.00179	0.00179	0.00179	0.00179	0.00179	0.00179
0.4	0.00179	0.00179	0.02500	0.06250	0.75000	0.10000	0.03750	0.00179	0.00179	0.00179	0.00179	0.00179	0.00179	0.00179	0.00179	0.00179	0.00179	0.00179	0.00179
0.5	0.00179	0.00179	0.00179	0.02500	0.06250	0.75000	0.10000	0.03750	0.00179	0.00179	0.00179	0.00179	0.00179	0.00179	0.00179	0.00179	0.00179	0.00179	0.00179
0.6	0.00014	0.00014	0.00014	0.00014	0.00200	0.00500	0.98000	0.00800	0.00300	0.00014	0.00014	0.00014	0.00014	0.00014	0.00014	0.00014	0.00014	0.00014	0.00014
0.7	0.00179	0.00179	0.00179	0.00179	0.00179	0.02500	0.06250	0.75000	0.10000	0.03750	0.00179	0.00179	0.00179	0.00179	0.00179	0.00179	0.00179	0.00179	0.00179
0.8	0.00179	0.00179	0.00179	0.00179	0.00179	0.00179	0.02500	0.06250	0.75000	0.10000	0.03750	0.00179	0.00179	0.00179	0.00179	0.00179	0.00179	0.00179	0.00179
0.9	0.00029	0.00029	0.00029	0.00029	0.00029	0.00029	0.00029	0.00400	0.01000	0.96000	0.01600	0.00600	0.00029	0.00029	0.00029	0.00029	0.00029	0.00029	0.00029
1	0.00179	0.00179	0.00179	0.00179	0.00179	0.00179	0.00179	0.00179	0.02500	0.06250	0.75000	0.10000	0.03750	0.00179	0.00179	0.00179	0.00179	0.00179	0.00179
1.1	0.00179	0.00179	0.00179	0.00179	0.00179	0.00179	0.00179	0.00179	0.00179	0.02500	0.06250	0.75000	0.10000	0.03750	0.00179	0.00179	0.00179	0.00179	0.00179
1.2	0.00071	0.00071	0.00071	0.00071	0.00071	0.00071	0.00071	0.00071	0.00071	0.00071	0.01000	0.02500	0.90000	0.04000	0.01500	0.00071	0.00071	0.00071	0.00071
1.3	0.00179	0.00179	0.00179	0.00179	0.00179	0.00179	0.00179	0.00179	0.00179	0.00179	0.00179	0.02500	0.06250	0.75000	0.10000	0.03750	0.00179	0.00179	0.00179
1.4	0.00071	0.00071	0.00071	0.00071	0.00071	0.00071	0.00071	0.00071	0.00071	0.00071	0.00071	0.00071	0.01000	0.02500	0.90000	0.04000	0.01500	0.00071	0.00071
1.5	0.00179	0.00179	0.00179	0.00179	0.00179	0.00179	0.00179	0.00179	0.00179	0.00179	0.00179	0.00179	0.00179	0.02500	0.06250	0.75000	0.10000	0.03750	0.00179
1.6	0.00143	0.00143	0.00143	0.00143	0.00143	0.00143	0.00143	0.00143	0.00143	0.00143	0.00143	0.00143	0.00143	0.00143	0.02000	0.05000	0.80000	0.08000	0.03000
1.7	0.00417	0.00417	0.00417	0.00417	0.00417	0.00417	0.00417	0.00417	0.00417	0.00417	0.00417	0.00417	0.00417	0.00417	0.00417	0.02500	0.06250	0.75000	0.10000
1.8	0.00813	0.00813	0.00813	0.00813	0.00813	0.00813	0.00813	0.00813	0.00813	0.00813	0.00813	0.00813	0.00813	0.00813	0.00813	0.00813	0.02000	0.05000	0.80000

Table 2. Mean residence time (hold time) as a function of the transition probability at the diagonal of the transition matrix, for Δt = 1s.

Transition probability	0.1	0.2	0.5	0.6	0.75	0.8	0.9	0.95
Mean residence time [s]	1.111	1.25	2	2.5	4	5	10	20

Transition probability	0.96	0.98	0.99	0.995	0.996	0.9967	0.998	0.999
Mean residence time [s]	25	50	100	200	250	300	500	1000

Table 3. Probabilities set for four values of the current density slope.

Slope [A/cm2/s]	-0.2	-0.1	+0.1	+0.2
Relative frequency	0.1	0.25	0.4	0.15

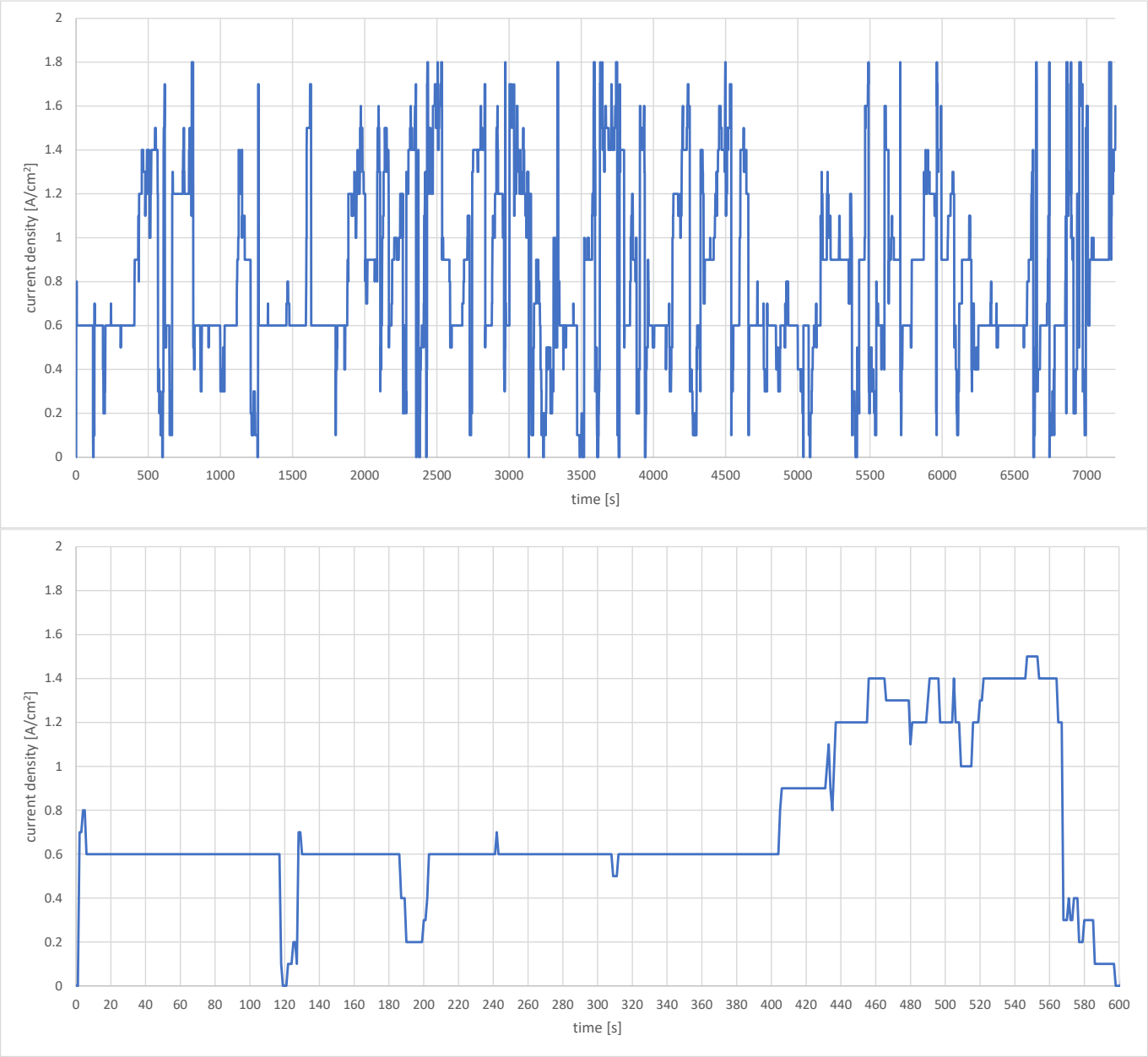

Figure 18. Upper: Markov chain stochastic process created with the transition matrix of Table 1. Lower: zoom-in on the first 600 s.

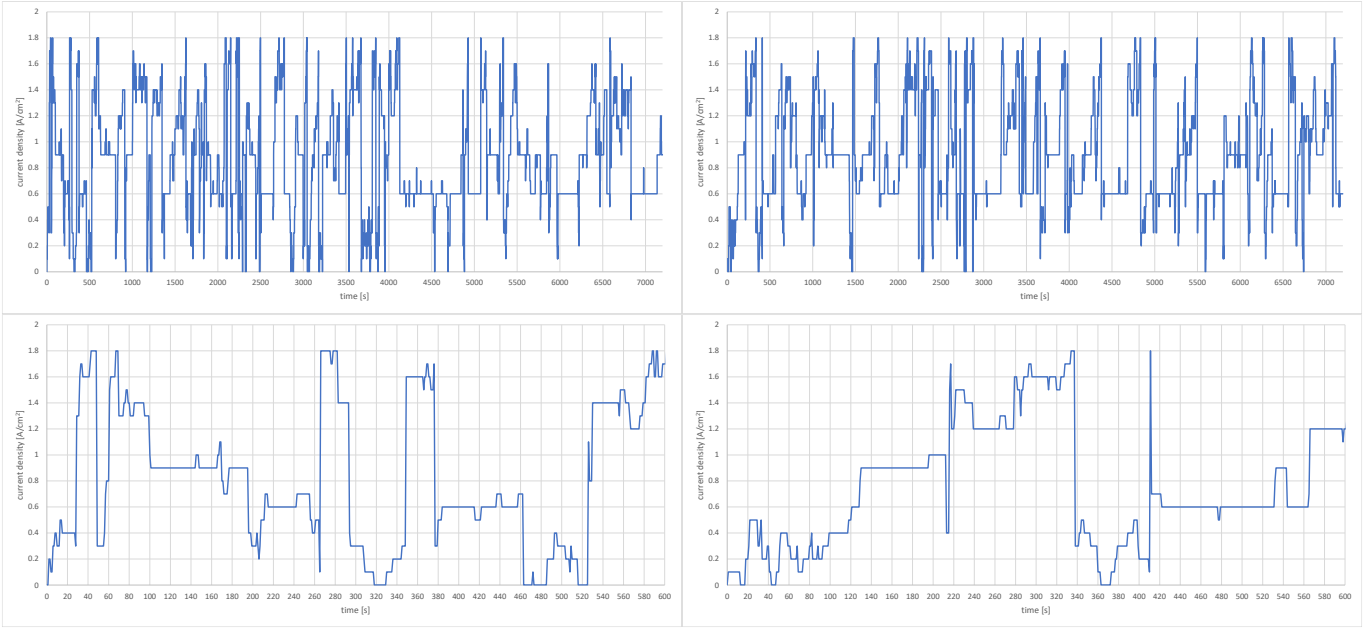

Figure 19. Other examples of MCADT profiles produced with the transition matrix of Table 1. Lower: zoom-in on the first 600 s.

3.2.2 Operating conditions in an MCADT

Up to this point only the current density has been discussed. However, it is important to define the behaviour of the other operating conditions. Rules such the ones shown in Figure 15 may be used. Generally, it is up to the designer of the experiment to decide how the test bench should respond given the dynamics of the load profile and the test bench's capability. In order to avoid starvation phenomena, it would probably be practical either to apply a feed-forward algorithm on the test bench automation system, or to predetermine the entire load profile and based on it predetermine the stream flows, pressures, temperatures and relevant humidity, again taking into account the response times of the test bench.

3.2.3 Steady-state (asymptotic) probabilities and minimum number of cycles[10]

Since MCADT are stochastic processes, the defined hold times must be seen as average values obtained asymptotically during running. It would be therefore of interest to understand what a minimum necessary number of transitions should be run – equivalently a minimum duration of the measurement campaign – where:

a) the expected hold times are asymptotically observed, and
b) all possible transitions are expected to appear

Point a) can be answered as follows. The steady-state probabilities of a Markov chain are calculated by solving the equation:

$$\pi = \pi P \tag{3.2}$$

[10] The author would like to acknowledge Prof. Andrea Casalegno who brought up this topic in a conference presentation of this approach [12].

This project has received funding from the Fuel Cells and Hydrogen 2 Joint Undertaking (now Clean Hydrogen Partnership) under grant agreement No 101006641. This Joint Undertaking receives support from the European Union's Horizon 2020 Research and Innovation programme, Hydrogen Europe and Hydrogen Europe Research.

where π is the array of steady-state probabilities and P is the transition matrix. The transition matrix of Table 1 has the steady-state probabilities shown in Table 4:

Table 4. Top row: current density levels [A/cm²]. Bottom row: steady state probabilities of the transition matrix of Table 1.

0	0.1	0.2	0.3	0.4	0.5	0.6	0.7	0.8	0.9	1	1.1	1.2	1.3	1.4	1.5	1.6	1.7	1.8
0.011	0.014	0.018	0.022	0.024	0.026	0.346	0.029	0.03	0.189	0.031	0.031	0.077	0.03	0.074	0.028	0.032	0.021	0.019

By multiplying the latter values with the diagonal of the transition matrix we obtain the absolute probabilities that each state (current density level) is repeated at the next transition. These values are given in Table 5:

Table 5. Top row: current density levels [A/cm²]. Bottom row: absolute probabilities of the transition matrix' diagonal.

0	0.1	0.2	0.3	0.4	0.5	0.6	0.7	0.8	0.9	1	1.1	1.2	1.3	1.4	1.5	1.6	1.7	1.8
0.009	0.010	0.013	0.015	0.017	0.019	0.322	0.021	0.021	0.172	0.022	0.022	0.066	0.022	0.064	0.020	0.024	0.015	0.015

The smallest probability in the table is 0.87%, the probability of having 0 A/cm^2. By inversing and multiplying with the transition time ($\Delta t = 1\ s$) we get the average time interval between appearances of 0 A/cm^2 $\tau_{i=0} \approx 115\ s$. It is then a question of how many times this interval should be repeated to reach an average of hold time equal to 5 s that Table 1 defines. This is a somewhat arbitrary decision. If 10 repetitions are chosen, then the necessary time is 1151. If the repetitions are 100 the time raises to 11512 s.

Similarly point b) above can be answered. This time the array of Table 4 must be multiplied with all columns of Table 1. The result is shown in Table 6. The minimum absolute probability is 0.311% leading to an average interval between repetitions $\tau_{i=0} \approx 32205\ s$. it is then up to the experimenter's discretion to decide the eventual number of repetitions as discussed before.

Table 6. Absolute probabilities of all transitions in Table 1.

current density before \ current density after	0	0.1	0.2	0.3	0.4	0.5	0.6	0.7	0.8	0.9	1	1.1	1.2	1.3	1.4	1.5	1.6	1.7	1.8
0	0.009	9E-04	3E-04	6E-05	6E-05	6E-05	6E-05	6E-05	6E-05	6E-05	6E-05	6E-05	6E-05	6E-05	6E-05	6E-05	6E-05	6E-05	6E-05
0.1	8E-04	0.01	0.001	5E-04	4E-05	4E-05	4E-05	4E-05	4E-05	4E-05	4E-05	4E-05	4E-05	4E-05	4E-05	4E-05	4E-05	4E-05	4E-05
0.2	4E-04	0.001	0.013	0.002	7E-04	3E-05	3E-05	3E-05	3E-05	3E-05	3E-05	3E-05	3E-05	3E-05	3E-05	3E-05	3E-05	3E-05	3E-05
0.3	4E-05	5E-04	0.001	0.015	0.002	8E-04	4E-05	4E-05	4E-05	4E-05	4E-05	4E-05	4E-05	4E-05	4E-05	4E-05	4E-05	4E-05	4E-05
0.4	4E-05	4E-05	6E-04	0.001	0.017	0.002	9E-04	4E-05	4E-05	4E-05	4E-05	4E-05	4E-05	4E-05	4E-05	4E-05	4E-05	4E-05	4E-05
0.5	4E-05	4E-05	4E-05	6E-04	0.002	0.019	0.002	9E-04	4E-05	4E-05	4E-05	4E-05	4E-05	4E-05	4E-05	4E-05	4E-05	4E-05	4E-05
0.6	5E-05	5E-05	5E-05	5E-05	7E-04	0.002	0.322	0.003	1E-03	5E-05	5E-05	5E-05	5E-05	5E-05	5E-05	5E-05	5E-05	5E-05	5E-05
0.7	5E-05	5E-05	5E-05	5E-05	5E-05	7E-04	0.002	0.021	0.003	0.001	5E-05	5E-05	5E-05	5E-05	5E-05	5E-05	5E-05	5E-05	5E-05
0.8	5E-05	5E-05	5E-05	5E-05	5E-05	5E-05	7E-04	0.002	0.021	0.003	0.001	5E-05	5E-05	5E-05	5E-05	5E-05	5E-05	5E-05	5E-05
0.9	5E-05	5E-05	5E-05	5E-05	5E-05	5E-05	5E-05	7E-04	0.002	0.172	0.003	0.001	5E-05	5E-05	5E-05	5E-05	5E-05	5E-05	5E-05
1	5E-05	5E-05	5E-05	5E-05	5E-05	5E-05	5E-05	5E-05	7E-04	0.002	0.022	0.003	0.001	5E-05	5E-05	5E-05	5E-05	5E-05	5E-05
1.1	5E-05	5E-05	5E-05	5E-05	5E-05	5E-05	5E-05	5E-05	5E-05	7E-04	0.002	0.022	0.003	0.001	5E-05	5E-05	5E-05	5E-05	5E-05
1.2	5E-05	5E-05	5E-05	5E-05	5E-05	5E-05	5E-05	5E-05	5E-05	5E-05	7E-04	0.002	0.066	0.003	0.001	5E-05	5E-05	5E-05	5E-05
1.3	5E-05	5E-05	5E-05	5E-05	5E-05	5E-05	5E-05	5E-05	5E-05	5E-05	5E-05	7E-04	0.002	0.022	0.003	0.001	5E-05	5E-05	5E-05
1.4	5E-05	5E-05	5E-05	5E-05	5E-05	5E-05	5E-05	5E-05	5E-05	5E-05	5E-05	5E-05	7E-04	0.002	0.064	0.003	0.001	5E-05	5E-05
1.5	5E-05	5E-05	5E-05	5E-05	5E-05	5E-05	5E-05	5E-05	5E-05	5E-05	5E-05	5E-05	5E-05	7E-04	0.002	0.02	0.003	0.001	5E-05
1.6	4E-05	4E-05	4E-05	4E-05	4E-05	4E-05	4E-05	4E-05	4E-05	4E-05	4E-05	4E-05	4E-05	4E-05	6E-04	0.002	0.024	0.002	9E-04
1.7	8E-05	8E-05	8E-05	8E-05	8E-05	8E-05	8E-05	8E-05	8E-05	8E-05	8E-05	8E-05	8E-05	8E-05	8E-05	5E-04	0.001	0.015	0.002
1.8	1E-04	1E-04	1E-04	1E-04	1E-04	1E-04	1E-04	1E-04	1E-04	1E-04	1E-04	1E-04	1E-04	1E-04	1E-04	1E-04	4E-04	9E-04	0.015

3.2.4 Application: transition matrices for the stack load profiles selected in Task 6.1 [1]

An interesting field to apply MCADT as described above are the four load profiles for stack testing produced in Task 6.1 of this work package (Figure 20) and later used to establish the LPT protocol in this project.

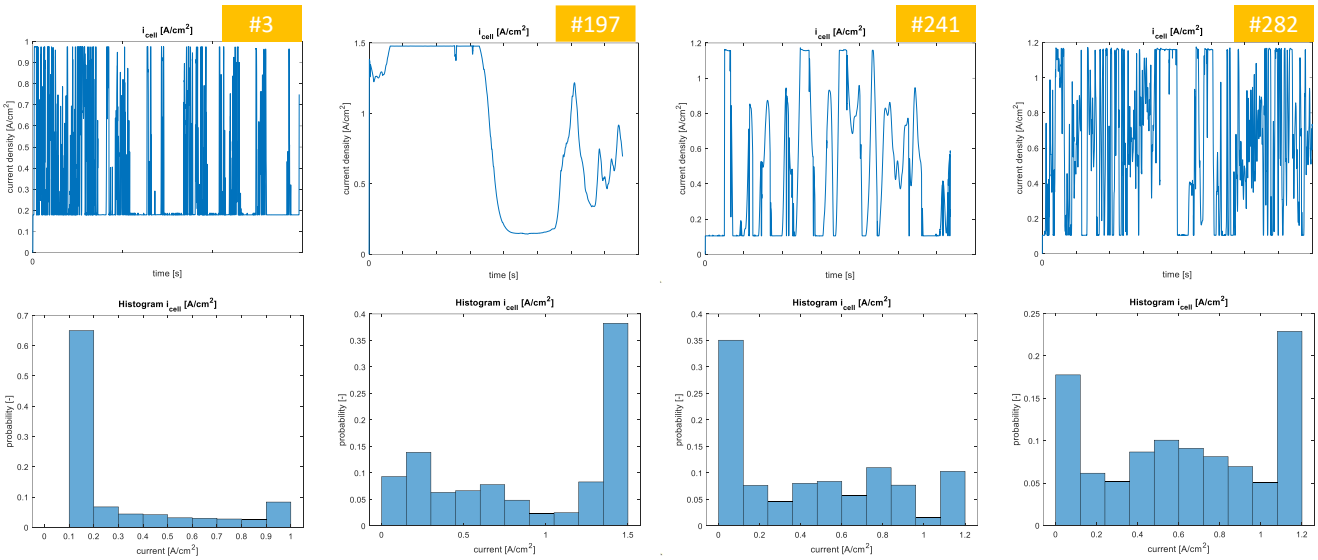

Figure 20. The four load profiles that were selected after simulations and shared with the WP2 partners [1] to produce new LPTs. The time scales vary.

The four current density profiles where statistically analysed, and the respective Markov chain transition matrices were produced (Table 7 up to Table 10).

In the transition matrices below, one can notice two issues. The first is that the transition probabilities are constrained to a small number of diagonals, leaving an important number of possible transitions with zero probability. This is against the approach of the method where an as broad as possible spectrum of transition values is desired. The second is that due to the difference in the time and current density resolution of the matrices and the original simulation data[11], transitions are aggregated, mainly in the matrix diagonal, leaving a very small probability for transition to other current densities. If the stochastic processes are deployed as described there, they will be led to behaviours quite different from the original load profiles.

Figure 21 is depicting the case #3 at three different time scales. Due to the small probability to transition from 1.0 to 0.9 A/cm^2, the process is "trapped" for long times at the maximum value.

Run #241 in Figure 22 is an extreme case where once the stack reaches 1.2 A/cm^2, it never leaves this state.

[11] The simulation data were extracted with 10 ms time resolution and continuous values for the current density.

Table 7. Transition matrix for run #3 with current density resolution 0.1 A/cm2 and time resolution 1s.

	0	0.1	0.2	0.3	0.4	0.5	0.6	0.7	0.8	0.9	1
0	0.60000	0.00000	0.40000	0.00000	0.00000	0.00000	0.00000	0.00000	0.00000	0.00000	0.00000
0.1	0.00000	0.00000	0.00000	1.00000	0.00000	0.00000	0.00000	0.00000	0.00000	0.00000	0.00000
0.2	0.00187	0.00269	0.99190	0.00230	0.00124	0.00000	0.00000	0.00000	0.00000	0.00000	0.00000
0.3	0.02647	0.00051	0.03174	0.88796	0.02724	0.02608	0.00000	0.00000	0.00000	0.00000	0.00000
0.4	0.02656	0.00061	0.00061	0.03792	0.87565	0.02825	0.03040	0.00000	0.00000	0.00000	0.00000
0.5	0.00000	0.03353	0.00038	0.00076	0.04363	0.83749	0.04858	0.03563	0.00000	0.00000	0.00000
0.6	0.00000	0.00775	0.02855	0.00066	0.00000	0.04073	0.80412	0.08765	0.03054	0.00000	0.00000
0.7	0.00000	0.00000	0.02430	0.00477	0.00023	0.00045	0.02498	0.82357	0.09650	0.02520	0.00000
0.8	0.00000	0.00000	0.00000	0.02439	0.00268	0.00000	0.00000	0.01153	0.83222	0.10158	0.02761
0.9	0.00000	0.00000	0.00000	0.00000	0.00959	0.01178	0.00027	0.00027	0.00548	0.83475	0.13785
1	0.00000	0.00000	0.00000	0.00000	0.00000	0.00000	0.00000	0.00000	0.00000	0.00019	0.99981

Table 8. Transition matrix for run #197 with current density resolution 0.1 A/cm2 and time resolution 1s.

	0	0.1	0.2	0.3	0.4	0.5	0.6	0.7	0.8	0.9	1	1.1	1.2	1.3	1.4	1.5
0	0.42857	0.57143	0.00000	0.00000	0.00000	0.00000	0.00000	0.00000	0.00000	0.00000	0.00000	0.00000	0.00000	0.00000	0.00000	0.00000
0.1	0.00000	0.99914	0.00072	0.00014	0.00000	0.00000	0.00000	0.00000	0.00000	0.00000	0.00000	0.00000	0.00000	0.00000	0.00000	0.00000
0.2	0.00000	0.00000	0.99927	0.00000	0.00073	0.00000	0.00000	0.00000	0.00000	0.00000	0.00000	0.00000	0.00000	0.00000	0.00000	0.00000
0.3	0.00000	0.00000	0.00000	0.99782	0.00000	0.00218	0.00000	0.00000	0.00000	0.00000	0.00000	0.00000	0.00000	0.00000	0.00000	0.00000
0.4	0.00000	0.00000	0.00000	0.00000	0.99787	0.00000	0.00213	0.00000	0.00000	0.00000	0.00000	0.00000	0.00000	0.00000	0.00000	0.00000
0.5	0.00000	0.00000	0.00000	0.00000	0.00000	0.99829	0.00000	0.00171	0.00000	0.00000	0.00000	0.00000	0.00000	0.00000	0.00000	0.00000
0.6	0.00000	0.00000	0.00000	0.00000	0.00000	0.00000	0.99856	0.00000	0.00144	0.00000	0.00000	0.00000	0.00000	0.00000	0.00000	0.00000
0.7	0.00000	0.00000	0.00000	0.00000	0.00000	0.00000	0.00000	0.99844	0.00000	0.00156	0.00000	0.00000	0.00000	0.00000	0.00000	0.00000
0.8	0.00000	0.00000	0.00000	0.00000	0.00000	0.00000	0.00000	0.00000	0.99779	0.00000	0.00221	0.00000	0.00000	0.00000	0.00000	0.00000
0.9	0.00000	0.00000	0.00000	0.00000	0.00000	0.00000	0.00000	0.00000	0.00000	0.99657	0.00000	0.00343	0.00000	0.00000	0.00000	0.00000
1	0.00000	0.00000	0.00000	0.00000	0.00000	0.00000	0.00000	0.00000	0.00000	0.00000	0.99441	0.00000	0.00559	0.00000	0.00000	0.00000
1.1	0.00000	0.00000	0.00000	0.00000	0.00000	0.00000	0.00000	0.00000	0.00000	0.00000	0.00000	0.99536	0.00000	0.00464	0.00000	0.00000
1.2	0.00000	0.00000	0.00000	0.00000	0.00000	0.00000	0.00000	0.00000	0.00000	0.00000	0.00000	0.00000	0.99691	0.00000	0.00309	0.00000
1.3	0.00000	0.00000	0.00000	0.00000	0.00000	0.00000	0.00000	0.00000	0.00000	0.00000	0.00039	0.00000	0.00058	0.99595	0.00212	0.00096
1.4	0.00000	0.00000	0.00000	0.00000	0.00000	0.00000	0.00000	0.00000	0.00000	0.00000	0.00000	0.00000	0.00000	0.00289	0.99339	0.00372
1.5	0.00000	0.00000	0.00000	0.00000	0.00000	0.00000	0.00000	0.00000	0.00000	0.00000	0.00000	0.00000	0.00000	0.00000	0.00015	0.99985

Table 9. Transition matrix for run #241 with current density resolution 0.1 A/cm2 and time resolution 1s.

	0	0.1	0.2	0.3	0.4	0.5	0.6	0.7	0.8	0.9	1	1.1	1.2
0	0.42857	0.57143	0.00000	0.00000	0.00000	0.00000	0.00000	0.00000	0.00000	0.00000	0.00000	0.00000	0.00000
0.1	0.00208	0.99539	0.00253	0.00000	0.00000	0.00000	0.00000	0.00000	0.00000	0.00000	0.00000	0.00000	0.00000
0.2	0.02180	0.00151	0.93794	0.03875	0.00000	0.00000	0.00000	0.00000	0.00000	0.00000	0.00000	0.00000	0.00000
0.3	0.01961	0.00449	0.00776	0.92034	0.04779	0.00000	0.00000	0.00000	0.00000	0.00000	0.00000	0.00000	0.00000
0.4	0.00000	0.01022	0.00349	0.00349	0.95618	0.02661	0.00000	0.00000	0.00000	0.00000	0.00000	0.00000	0.00000
0.5	0.00000	0.00000	0.00482	0.00221	0.00181	0.97711	0.01405	0.00000	0.00000	0.00000	0.00000	0.00000	0.00000
0.6	0.00000	0.00000	0.00000	0.00413	0.00236	0.00207	0.97608	0.01536	0.00000	0.00000	0.00000	0.00000	0.00000
0.7	0.00000	0.00000	0.00000	0.00000	0.00312	0.00156	0.00052	0.98545	0.00935	0.00000	0.00000	0.00000	0.00000
0.8	0.00000	0.00000	0.00000	0.00000	0.00000	0.00051	0.00017	0.00253	0.99190	0.00489	0.00000	0.00000	0.00000
0.9	0.00000	0.00000	0.00000	0.00000	0.00000	0.00000	0.00122	0.00049	0.00585	0.98805	0.00439	0.00000	0.00000
1	0.00000	0.00000	0.00000	0.00000	0.00000	0.00000	0.00000	0.00534	0.00000	0.02244	0.95513	0.01175	0.00534
1.1	0.00000	0.00000	0.00000	0.00000	0.00000	0.00000	0.00000	0.00000	0.01644	0.00137	0.00411	0.93973	0.03836
1.2	0.00000	0.00000	0.00000	0.00000	0.00000	0.00000	0.00000	0.00000	0.00000	0.00000	0.00000	0.00000	1.00000

Table 10. Transition matrix for run #282 with current density resolution 0.1 A/cm2 and time resolution 1s.

	0	0.1	0.2	0.3	0.4	0.5	0.6	0.7	0.8	0.9	1	1.1	1.2
0	0.42857	0.57143	0.00000	0.00000	0.00000	0.00000	0.00000	0.00000	0.00000	0.00000	0.00000	0.00000	0.00000
0.1	0.00112	0.99764	0.00124	0.00000	0.00000	0.00000	0.00000	0.00000	0.00000	0.00000	0.00000	0.00000	0.00000
0.2	0.00578	0.00108	0.98345	0.00969	0.00000	0.00000	0.00000	0.00000	0.00000	0.00000	0.00000	0.00000	0.00000
0.3	0.00536	0.00089	0.00238	0.98467	0.00670	0.00000	0.00000	0.00000	0.00000	0.00000	0.00000	0.00000	0.00000
0.4	0.00000	0.00121	0.00086	0.00199	0.99360	0.00234	0.00000	0.00000	0.00000	0.00000	0.00000	0.00000	0.00000
0.5	0.00000	0.00000	0.00105	0.00038	0.00369	0.99187	0.00301	0.00000	0.00000	0.00000	0.00000	0.00000	0.00000
0.6	0.00000	0.00000	0.00000	0.00084	0.00051	0.00287	0.99071	0.00507	0.00000	0.00000	0.00000	0.00000	0.00000
0.7	0.00000	0.00000	0.00000	0.00000	0.00096	0.00032	0.00184	0.98991	0.00697	0.00000	0.00000	0.00000	0.00000
0.8	0.00000	0.00000	0.00000	0.00000	0.00000	0.00155	0.00000	0.00106	0.98752	0.00987	0.00000	0.00000	0.00000
0.9	0.00000	0.00000	0.00000	0.00000	0.00000	0.00000	0.00158	0.00000	0.00106	0.98500	0.01236	0.00000	0.00000
1	0.00000	0.00000	0.00000	0.00000	0.00000	0.00000	0.00000	0.00133	0.00000	0.00089	0.98445	0.01259	0.00074
1.1	0.00000	0.00000	0.00000	0.00000	0.00000	0.00000	0.00000	0.00000	0.00246	0.00037	0.00012	0.97956	0.01748
1.2	0.00000	0.00000	0.00000	0.00000	0.00000	0.00000	0.00000	0.00000	0.00000	0.00000	0.00000	0.00003	0.99997

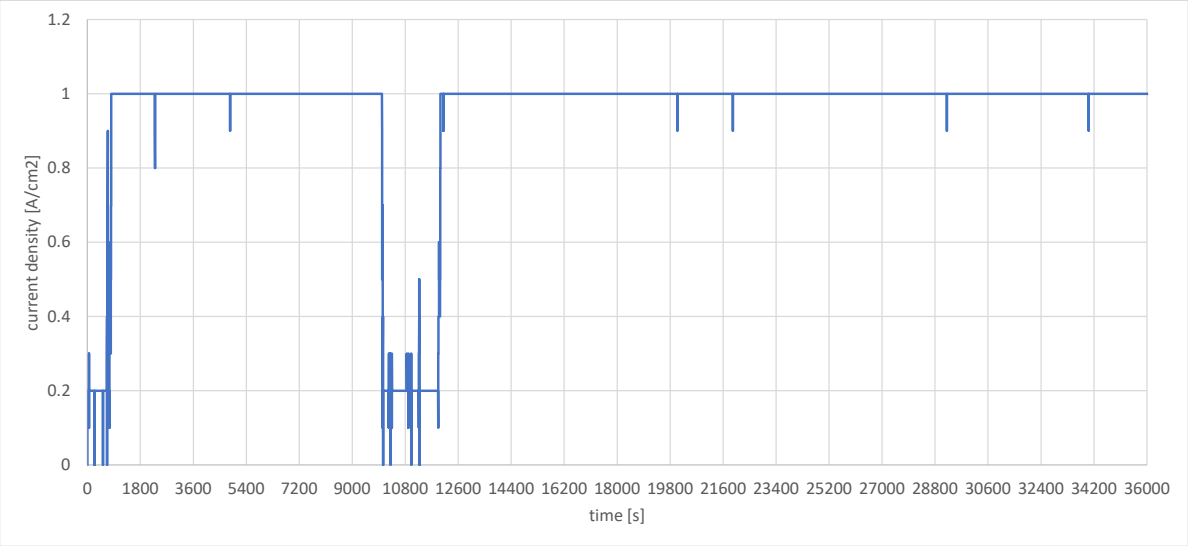

Figure 21. Run case #3 deployed as a Markov chain stochastic process according to the transition matrix of Table 7.

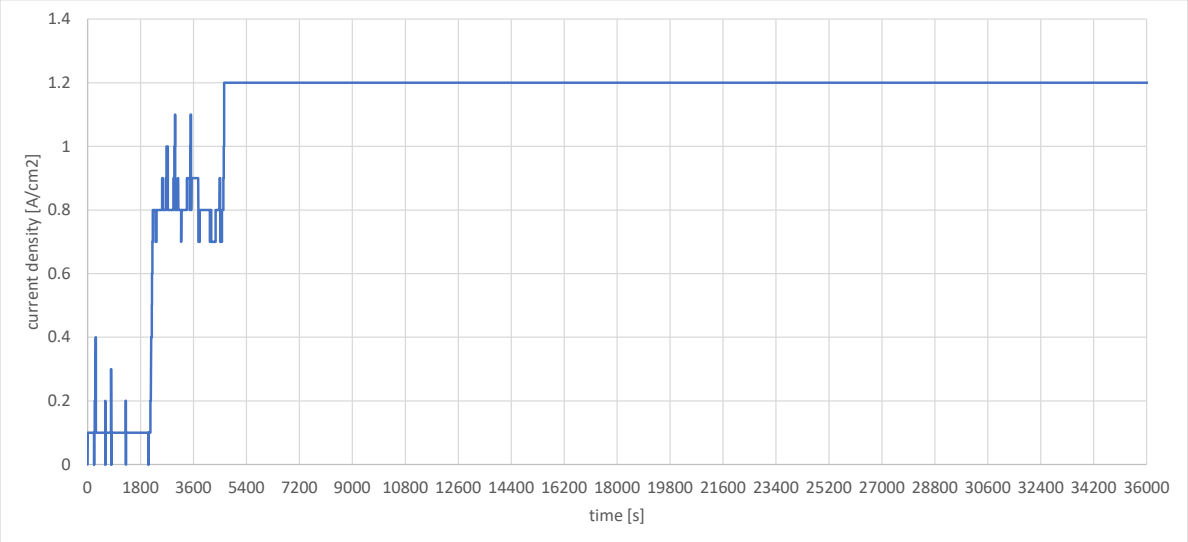

Figure 22. Run case #241 deployed as a Markov chain stochastic process according to the transition matrix of Table 9.

This project has received funding from the Fuel Cells and Hydrogen 2 Joint Undertaking (now Clean Hydrogen Partnership) under grant agreement No 101006641. This Joint Undertaking receives support from the European Union's Horizon 2020 Research and Innovation programme, Hydrogen Europe and Hydrogen Europe Research.

In order to remedy this issue, the transition matrices are transformed according to the following formula:

$$p_{i,j}^{new} = p_{i,j}(1-\alpha) + \frac{\alpha}{N} \quad (3.3)$$

where:

- $p_{i,j}^{new}$ is the new probability of transition from state i to state j,
- $p_{i,j}$ is the original probability of transition from state i to state j,
- is a factor named here "acceleration factor" with $0 \leq \alpha \leq 1$
- N is the number of transitions in the transition matrix

It is easily shown that $\sum_{j=1}^{N} p_{i,j}^{new} = 1$ for all j.

This transformation is adding probabilities to all transitions in the matrix. At the same time it is reducing the values that originally were >0 by the factor $(1-\alpha)$. The higher the factor α, the more abrupt the transitions and the smaller the hold times in the stochastic processes. This can be seen in Figure 23, where three different acceleration factors are compared (α=0.01, 0.02 and 0.05).

Finally, Figure 24 up to Figure 27 are depicting the four run cases produced as stochastic processes from the same transition matrices with acceleration factor α = 0.05.

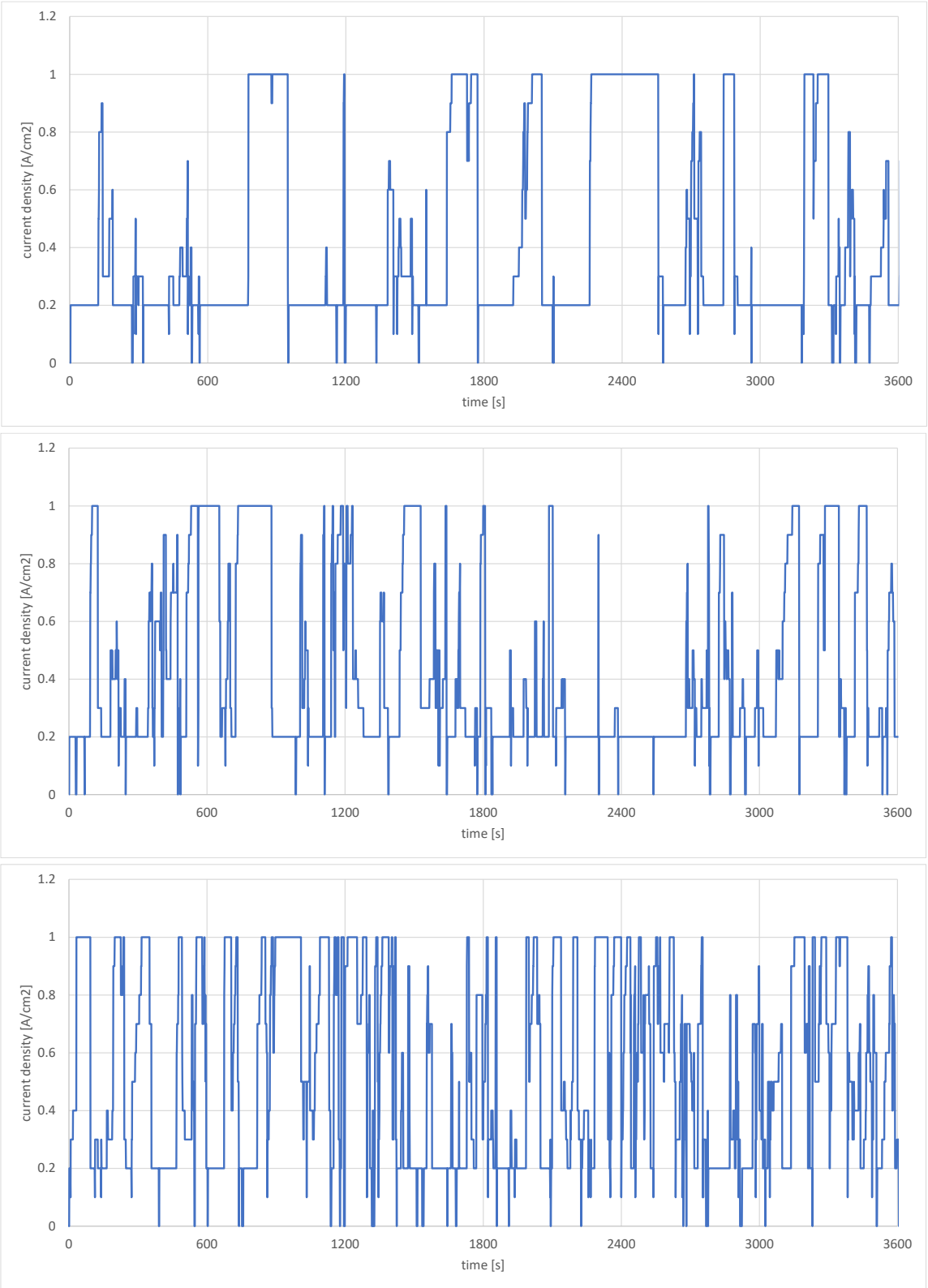

Figure 23. Run case #3 deployed as a Markov chain stochastic process according to the transition matrix of Table 7 transformed with acceleration factor α=0.01 (top), α=0.02 (middle), α=0.05 (bottom).

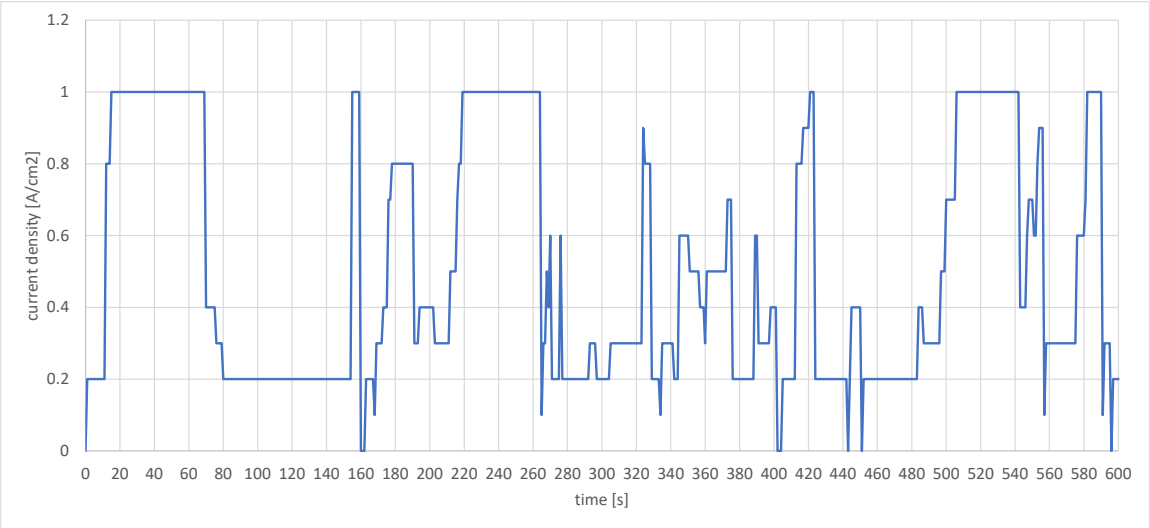

Figure 24. Run case #3 deployed as a Markov chain stochastic process according to the transition matrix of Table 7 and acceleration factor α = 0.05.

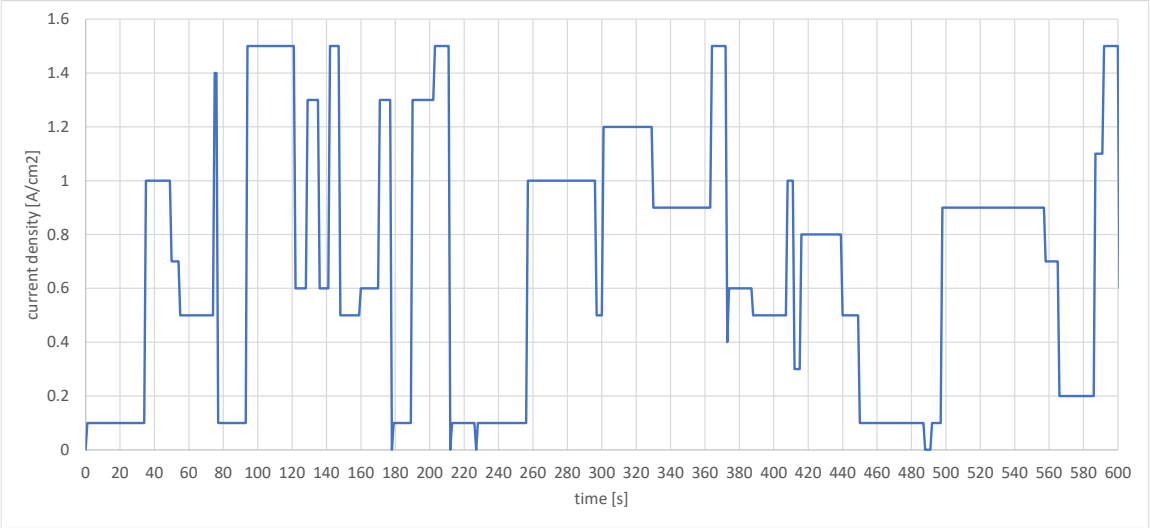

Figure 25. Run case #197 deployed as a Markov chain stochastic process according to the transition matrix of Table 8 and acceleration factor α = 0.05.

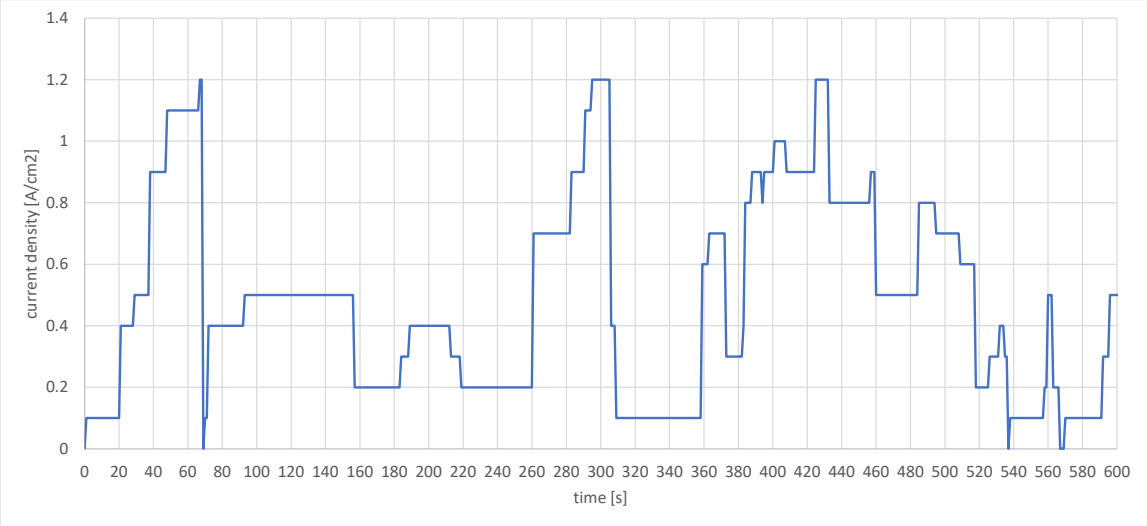

Figure 26. Run case #241 deployed as a Markov chain stochastic process according to the transition matrix of Table 9 and acceleration factor α = 0.05.

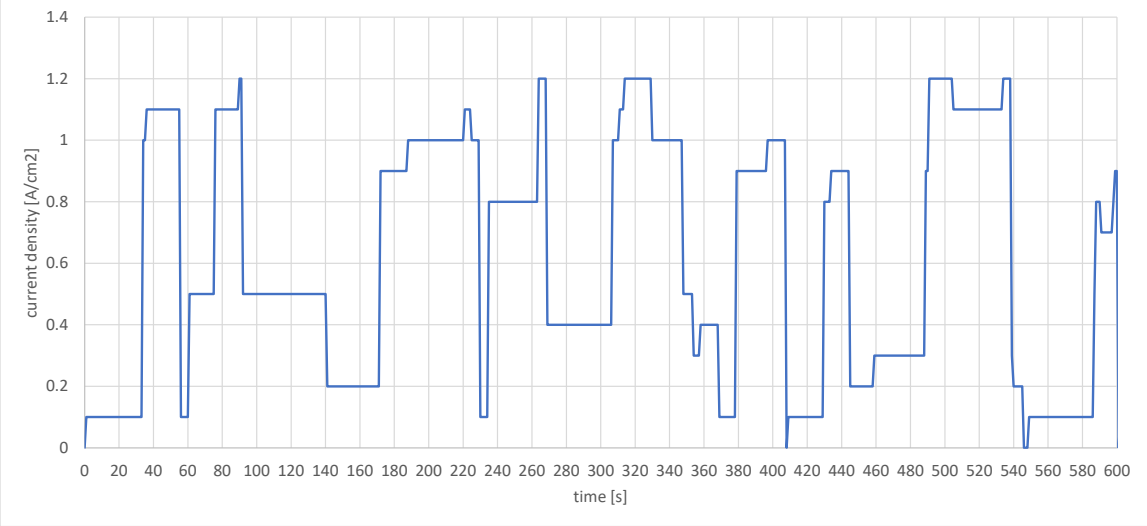

Figure 27. Run case #282 deployed as a Markov chain stochastic process according to the transition matrix of Table 10 and acceleration factor α = 0.05.

3.2.5 Application II: Throughput and dynamic throughput in the MCADT

An interesting property of the MCADT is that the dynamic throughput of the current density does not correlate strongly with the throughput. Indeed, Figure 28 is juxtaposing the throughput and the dynamic throughput for 38 MCADT profiles created based on the transition matrix of Table 1. The duration of each was 10 hours. Although there is a linear relation between the two magnitudes, a linear regression is not explaining all variation. The coefficient of determination (R2) is only 0.321. Moreover, the Pearson correlation coefficient is 0.567.

This property has an important impact on designing experiments using MCADT. By changing the probabilities in the MCADT transition matrix as discussed in §3.2.1 an experimenter can differentiate the

throughput of a series of measurements. By creating new series of measurement points, as done for Figure 28, each new series will have a similar throughput and a very loosely correlated dynamic throughput. This means that no excessive additional effort needs to be put to create variability on the dynamic throughput. Its variability is inherent.

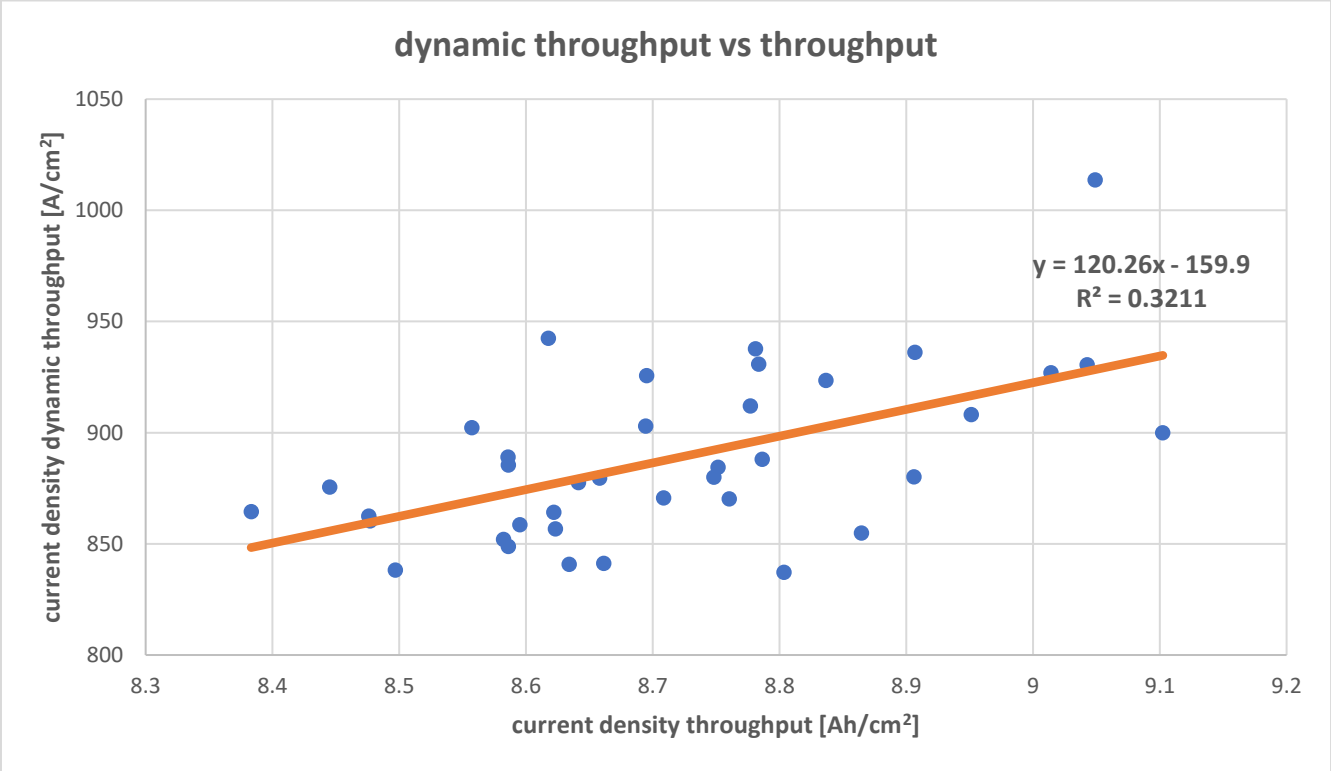

Figure 28. Current density dynamic throughput vs. throughput.

This project has received funding from the Fuel Cells and Hydrogen 2 Joint Undertaking (now Clean Hydrogen Partnership) under grant agreement No 101006641. This Joint Undertaking receives support from the European Union's Horizon 2020 Research and Innovation programme, Hydrogen Europe and Hydrogen Europe Research.

4 CONCLUSION AND FUTURE WORK

In this report two results of interest, from both industrial and academic perspectives, are presented. The first is a statistical modelling approach for forecasting of fuel cells' degradation. The second is an alternative approach for accelerated testing which, when ran, offers a richer spectrum of information on how the various stressors impact performance and degradation.

As far as the discussed modelling approach is concerned, the more important learnings are not the models themselves, rather the discussed criteria on how one should distinguish good and less good models. It was shown how one can be easily misled and in the end use very erroneous models leading to very wrong conclusions. Selecting the appropriate model is as much an art as developing the models themselves and further work on the relevant criteria must be done and discussed.

Beyond the latter, other work that can be done in modelling are technical improvements such as:

- Further exploration of modelling possibilities whether within the family of linear models or other machine learning techniques,
- Refinement of the models by elimination of statistically not significant coefficients,
- Use of alternative optimisation approaches for linear models, such as Ridge, Lasso, Least Angle, etc.,
- Apply L1 optimisation, i.e., minimisation of the sum of absolute residuals, rather than their squares, which would be more appropriate for the distribution of the residual.

As regards the Markov chain accelerated durability testing, it lacks experimental trials and its drawbacks in practice need to be examined and discussed. Challenges in the laboratory implementation are expected, mainly due to starvation that may be induced if the oxidant/fuel are not sufficient during the intense and randomised cycle dynamics. For this reason, the experiments need to be carefully designed. Furthermore, we need to understand the impact of different configurations of the transition matrix on the duration of accelerated tests and the quality of the learnings, including the development of statistical models.

In general, both topics have considerable potential for improvement and learning that will hopefully help us understand fuel cells degradation better and contribute to the optimisation of their use especially in their industrial and commercial use.

This project has received funding from the Fuel Cells and Hydrogen 2 Joint Undertaking (now Clean Hydrogen Partnership) under grant agreement No 101006641. This Joint Undertaking receives support from the European Union's Horizon 2020 Research and Innovation programme, Hydrogen Europe and Hydrogen Europe Research.

5 REFERENCES

[1] IMMORTAL WP6 deliverable report D6.1 – Initial data from fuel cell HD trucks providing load frequency distribution (https://immortal-fuelcell.eu/index.php/activities/delivrables#wp6)

[2] https://www.h2haul.eu/

[3] IMMORTAL project proposal, Nr. SEP-210656636, p. 83

[4] IMMORTAL WP2 deliverable report D2.3 – Second end-of-testing analysis of initial HD-specific MEAs (https://immortal-fuelcell.eu/index.php/activities/delivrables#wp2)

[5] https://en.wikipedia.org/wiki/Multicollinearity

[6] Probabilistic Machine Learning, lecture 7 – parametric regression, slide 4. Video recordings of Prof. Philipp Henning at the University of Tübingen. (https://youtu.be/riZ-B8y14qE?si=9a5JRyO1kWsjkcsR, https://github.com/philipphennig/Probabilistic_ML/tree/main/slides).

[7] L. Tsikonis, S. Diethelm, H. Seiler, A. Nakajo, J. Van herle, D. Favrat, *Investigating Reliability on Fuel Cell Model Identification. Part II: An Estimation Method for Stochastic Parameters*, Fuel Cells 2012, 5, 685 (https://doi.org/10.1002/fuce.201200031).

[8] M. H. Kutner, Ch. J. Nachtsheim, J. Neter, *Applied Linear Regression Models*, fourth edition, McGraw-Hill, 2004.

[9] A. Dean, D. Voss, D. Draguljić, *Design and Analysis of Experiments*, second edition, Springer International Publishing, 2017.

[10] M. Koprek, R. Schlumberger, F. Wilhelm, J. Scholta, M. Hölzle, *Development and Evaluation of Accelerated Durability Tests Under Realistic Operating Conditions for PEMFC Stacks – a Systematic Approach*, presentation I01B-1846, ECS 244th Meeting 2023, Gothenburg, Sweden (https://ecs.confex.com/ecs/244/meetingapp.cgi/Paper/177844).

[11] https://en.wikipedia.org/wiki/Markov_chain

[12] L. Tsikonis, *Load Profile Test Development and Analysis from Heavy Duty Truck Drive Cycles*, presentation I01Z-2162, ECS 244th Meeting 2023, Gothenburg, Sweden (https://ecs.confex.com/ecs/244/meetingapp.cgi/Paper/176998).

[13] https://en.wikipedia.org/wiki/Intensive_and_extensive_properties

This project has received funding from the Fuel Cells and Hydrogen 2 Joint Undertaking (now Clean Hydrogen Partnership) under grant agreement No 101006641. This Joint Undertaking receives support from the European Union's Horizon 2020 Research and Innovation programme, Hydrogen Europe and Hydrogen Europe Research.

6 APPENDIX A: CORRECTION IN THE DEFINITION OF DYNAMIC THROUGHPUT

In the Appendix A of D6.1, the first deliverable of WP6 [1], the dynamic throughput was defined as an intensive magnitude, i.e. a magnitude that does not depend on the duration of the load profile [13]. This was senseful for uses such as the comparison of load profiles of different duration, as done in D6.1. However, another intensive magnitude was available and finally used in the selection process for load profiles, namely the normalised dynamic throughput, that is, the dynamic throughput normalised over the average value of the considered magnitude.

Furthermore, an extensive definition of the dynamic throughput, i.e., a definition that depends on the duration of the mission is very useful when one wishes to relate the dynamics of a load profile with the fuel cell's degradation. In this case the longer the duration of the testing, the longer the impact of the dynamic behaviour – expressed by its metric, the dynamic throughput – on the fuel cell's degradation and generally its durability. This approach was extensively applied for the creation and use of the degradation model of section 2 (A fuel cell degradation model for durability forecasting).

On the other hand, the metric as defined in the Appendix A of D6.1 [1] may be considered its specific version, i.e., the dynamic throughput per time unit.

Therefore, the definitions in the following frame are proposed. In the case of the normalised dynamic throughput, the absolute value of the magnitude is used, in order to extend its use to batteries or other applications where the magnitude, e.g., the current, may have negative values.

T_{tot} is the total time duration of the measurement.

$$dynamic\ throughput = \int_0^{T_{tot}} \left| \frac{d}{dt} magnitude \right| \cdot dt \tag{A.1}$$

$$specific\ dynamic\ throughput = \frac{1}{T_{tot}} \int_0^{T_{tot}} \left| \frac{d}{dt} magnitude \right| \cdot dt \tag{A.2}$$

$$normalised\ dynamic\ throughput = \frac{\int_0^{T_{tot}} \left| \frac{d}{dt} magnitude \right| \cdot dt}{\int_0^{T_{tot}} |magnitude| \cdot dt} \tag{A.3}$$

This project has received funding from the Fuel Cells and Hydrogen 2 Joint Undertaking (now Clean Hydrogen Partnership) under grant agreement No 101006641. This Joint Undertaking receives support from the European Union's Horizon 2020 Research and Innovation programme, Hydrogen Europe and Hydrogen Europe Research.

7 APPENDIX B: ADAPTATION OF THE FORMULA CALCULATING THE VARIANCE OF VALUES PREDICTED FROM THE MODEL

According to [8], the following formula should be used for the calculation of the variance of a value predicted from the model:

$$s^2\{prediction\} = MSE_{train} + s^2\{\hat{Y}_h\} = MSE_{train}[1 + \Phi_h'(\Phi'\Phi)^{-1}\Phi_h] \quad \text{(B.1)}$$

where:

- $\hat{Y}_h$ is a value predicted from the model.
- $s^2\{\hat{Y}_h\}$ is the variance of the sampling distribution of $\hat{Y}_h$.
- Φ_h is the array of the features' values (1xp matrix) used in the regression for the calculation of $\hat{Y}_h$ (see also §2.1.2 and Figure 4).
- Φ is the Nxp matrix of the N data points with p features used for the model training.
- $s^2\{prediction\}$ is the variance of the model predicted value.
- $MSE_{train}$is the mean squared error from the model training[12]

The term $\Phi_h'(\Phi'\Phi)^{-1}\Phi_h$ is also called "hat value" of the new point:

$$h_h = \Phi_h'(\Phi'\Phi)^{-1}\Phi_h$$

and it is a measure of the "distance" of a predicted value from the centroid of the training data and consequently a measure of extrapolation from the model training region. Figure 29 is a graphical depiction of this notion.

Therefore, equation (B.1) can be rewritten as:

$$s^2\{prediction\} = MSE_{train}[1 + h_h] \quad \text{(B.2)}$$

For the training data, the "hat matrix" is the NxN matrix defined as:

$$H = \Phi(\Phi'\Phi)^{-1}\Phi'$$

Its diagonal elements are the hat values of the measurement points used for the model training. They have the following properties:

$$0 \leq h_{ii} \leq 1$$

$$\sum_{i=1}^{N} h_{ii} = p$$

$$\bar{h} = \frac{p}{N}$$

were:

- p is the number of features of the model and
- $\bar{h}$ is the average "hat value" of all data points used for the model training

[12] In this application the MSE from the test data was used, which essentially was equal to the training error

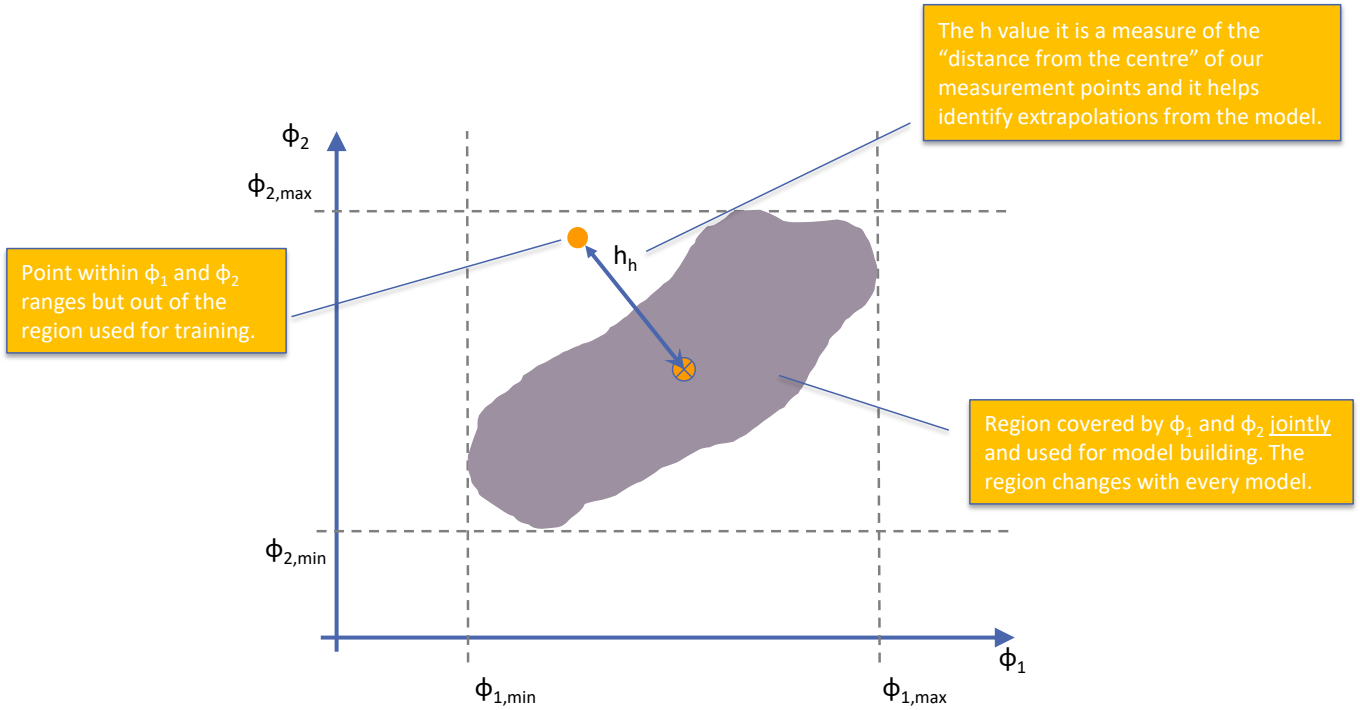

Figure 29. The "hat value" is a measure of a predicted model's extrapolation. Schematic adapted from [8], p.231.

One issue with equation (B.2) is that it is taking into consideration only the absolute value of the hat values. This means that, if the number of training points is high, as is the case in this application, where the order of magnitude of the average hat value $\bar{h}$ is 1x10^{-5}, any extrapolation from the model, even if it had a hat value 100 times higher than the average of the training points, i.e.: $h_h = 100\bar{h}$, the impact of this extrapolation to the prediction variance would be minimal. This does not make practical sense and it underestimates considerably the prediction error under high extrapolation.

For this reason, the author proceeded to the following adaptation of the formula:

$$s^2\{prediction\} = MSE_{train}\frac{h_h}{\bar{h}}[1 + h_h] \quad \text{(B.3)}$$

which is finally presented in §2.1.4, p.9. This is based on the idea that the MSE_{train} is an average expressing the average distance (hat value $\bar{h}$) of all training data points from their training centroid. The author maintains that the original calculation of the variance according to equation (B.1) is erroneous, namely the assumption that the variance of the distribution of any given $\hat{Y}_h$ at $\Phi_h = \Phi_{(X_h)}$, given input $X = X_h$ is constant and equal to MSE_{train} and it is independent of the distance to the training centroid ([8], p.58). Equation (B.3) is an approximation attempting to reflect the impact of the distance of a new data point from the training centroid.

Practically, this adaptation has the advantage to be accounting for the order of magnitude of the hat values. That is, if the h_h is in the order of magnitude of the training points (order of magnitude of $\bar{h}$), then the fraction has smaller impact compared to the term in brackets. If the extrapolation is relatively high not in absolute rather in relative terms, i.e., if h_h is 100 times larger than $\bar{h}$, then the prediction variance if mainly impacted by the fraction in (B.3).

Finally, to be noted that this approach is consistent with the general knowledge that the confidence band in linear regression is hyperbolic because it is proportional to the square root of the distance from the training centroid (Figure 30).

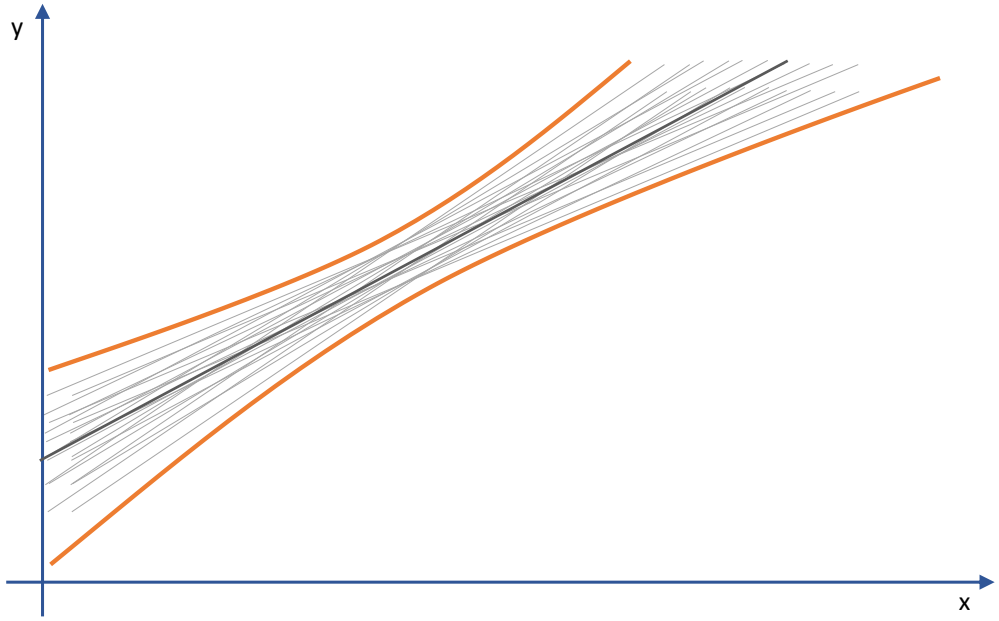

Figure 30. The confidence interval (orange) is due to the uncertainty in the regression coefficients. Here an example of a simple linear regression with variations on the intercept and the slope. The interval is hyperbolic as a function to the distance of x from the training data centroid.